UNIVERSIDAD DE INVESTIGACIÓN DE TECNOLOGÍA EXPERIMENTAL YACHAY

Escuela de Ciencias Físicas y Nanotecnología

TÍTULO: Optical Characterization of Graphene Multi-layers on SiO$_2$

Trabajo de integración curricular presentado como requisito para la obtención
del título de ingeniero en Nanotecnología

Autor:

Xavier Alexander López Loaiza

Tutor:

Dr. rer Nat. Julio Cesar Chacón Torres

Urcuquí, Agosto 2022

Urcuquí, 11 de agosto de 2022

SECRETARÍA GENERAL
ESCUELA DE CIENCIAS FÍSICAS Y NANOTECNOLOGÍA
CARRERA DE NANOTECNOLOGÍA
ACTA DE DEFENSA No. UITEY-PHY-2022-00015-AD

En la ciudad de San Miguel de Urcuquí, Provincia de Imbabura, a los 11 días del mes de agosto de 2022, a las 11:00 horas, en el Aula S_CAN de la Universidad de Investigación de Tecnología Experimental Yachay y ante el Tribunal Calificador, integrado por los docentes:

Presidente Tribunal de Defensa	Dra. BRICEÑO ARAUJO, SARAH ELISA , Ph.D.
Miembro No Tutor	Dra. PERALTA ARCIA, MAYRA ALEJANDRA DE JESUS , Ph.D.
Tutor	Dr. CHACON TORRES, JULIO CESAR , Ph.D.

Se presenta el(la) señor(ita) estudiante **LOPEZ LOAIZA, XAVIER ALEXANDER**, con cédula de identidad No. **1722108055**, de la **ESCUELA DE CIENCIAS FÍSICAS Y NANOTECNOLOGÍA**, de la Carrera de **NANOTECNOLOGÍA**, aprobada por el Consejo de Educación Superior (CES), mediante Resolución **RPC-SO-13-No.156-2015**, con el objeto de rendir la sustentación de su trabajo de titulación denominado: **OPTICAL CHARACTERIZATION OF GRAPHENE MULTI-LAYERS ON SI02**, previa a la obtención del título de **INGENIERO/A EN NANOTECNOLOGÍA**.

El citado trabajo de titulación, fue debidamente aprobado por el(los) docente(s):

Tutor	Dr. CHACON TORRES, JULIO CESAR , Ph.D.

Y recibió las observaciones de los otros miembros del Tribunal Calificador, las mismas que han sido incorporadas por el(la) estudiante.

Previamente cumplidos los requisitos legales y reglamentarios, el trabajo de titulación fue sustentado por el(la) estudiante y examinado por los miembros del Tribunal Calificador. Escuchada la sustentación del trabajo de titulación, que integró la exposición de el(la) estudiante sobre el contenido de la misma y las preguntas formuladas por los miembros del Tribunal, se califica la sustentación del trabajo de titulación con las siguientes calificaciones:

Tipo	Docente	Calificación
Presidente Tribunal De Defensa	Dra. BRICEÑO ARAUJO, SARAH ELISA , Ph.D.	10,0
Miembro Tribunal De Defensa	Dra. PERALTA ARCIA, MAYRA ALEJANDRA DE JESUS , Ph.D.	9,5
Tutor	Dr. CHACON TORRES, JULIO CESAR , Ph.D.	10,0

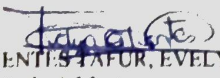Lo que da un promedio de: **9.8 (Nueve punto Ocho)**, sobre 10 (diez), equivalente a: **APROBADO**

Para constancia de lo actuado, firman los miembros del Tribunal Calificador, el/la estudiante y el/la secretario ad-hoc.

LOPEZ LOAIZA, XAVIER ALEXANDER
Estudiante

Dra. BRICEÑO ARAUJO, SARAH ELISA , Ph.D.
Presidente Tribunal de Defensa

Dr. CHACON TORRES, JULIO CESAR , Ph.D.
Tutor

Dra. PERALTA ARCIA, MAYRA ALEJANDRA DE JESUS , Ph.D.
Miembro No Tutor

CIFUENTES TAFUR, EVELYN CAROLINA
Secretario Ad-hoc

AUTORÍA

Yo, Xavier Alexander López Loaiza, con cédula de identidad 1722108055, declaro que las ideas, juicios, valoraciones, interpretaciones, consultas bibliográficas, definiciones y conceptualizaciones expuestas en el presente trabajo; así cómo, los procedimientos y herramientas utilizadas en la investigación, son de absoluta responsabilidad de el/la autora (a) del trabajo de integración curricular. Así mismo, me acojo a los reglamentos internos de la Universidad de Investigación de Tecnología Experimental Yachay.

Urcuquí, Agosto 2022.

Firmado electrónicamente por:
XAVIER ALEXANDER LOPEZ LOAIZA

_____
Xavier Alexander López Loaiza
CI: 1722108055

AUTORIZACIÓN DE PUBLICACIÓN

Yo, Xavier Alexander López Loaiza**,** con cédula de identidad 1722108055, cedo a la Universidad de Investigación de Tecnología Experimental Yachay, los derechos de publicación de la presente obra, sin que deba haber un reconocimiento económico por este concepto. Declaro además que el texto del presente trabajo de titulación no podrá ser cedido a ninguna empresa editorial para su publicación u otros fines, sin contar previamente con la autorización escrita de la Universidad.

Asimismo, autorizo a la Universidad que realice la digitalización y publicación de este trabajo de integración curricular en el repositorio virtual, de conformidad a lo dispuesto en el Art. 144 de la Ley Orgánica de Educación Superior

Urcuquí, Agosto 2022.

Firmado electrónicamente por:
**XAVIER
ALEXANDER
LOPEZ LOAIZA**

_____
Xavier Alexander López Loaiza
CI: 1722108055

Acknowledgements

Abstract

Graphene is a revolutionary material that brought numerous modern applications in many fields of industry. Additionally, it presents some properties that enable its use in many electronic devices. As a consequence, the control of the properties, which varies depending on its synthesis, is considered an important factor in its efficiency. For this purpose, the characterization of this material is extremely important because between all the features we can obtain, the number of layers is going to dictate a few principal properties over the material. Thus, in order to identify the number of layers of a graphene flake, it is necessary to apply two main techniques. In general, there are several characterization methods that can help us to complete this task, however, we are going to use and implement two of them. These techniques are optical contrast analysis and Raman spectroscopy. Although the optical contrast analysis is considered the simplest technique to determine the number of layers of 2D materials, it is very easy to use due to the employment of free software (ImageJ) accompanied with good results. On the other hand, Raman spectroscopy could be hard to implement, which cannot differentiate between two or more layers present in the material and uses complicated laboratory equipment. Nevertheless, Raman spectroscopy is going to be utilized in this work to complement the results obtained from the optical contrast analysis. The main objective of this work is to be able to identify the number of layers using the method of optical contrast analysis that can be reproducible in every computer due to the open software it uses. Therefore, this work will contribute to the determination of the number of layers for any 2D material making the use of a simple method presented here.

Keywords: Electronics, Spectroscopy, 2D Materials, ImageJ, Substrate.

Resumen

El grafeno es un material revolucionario que ha traido numerosas aplicaciones modernas en muchos campos de la industria. Adicionalmente, presenta algunas propiedades que lo llevan a ser usado en algunos dispositivos electrónicos. Cómo consecuencia, el poder de controlar sus propiedades, que depende en mayor parte de la síntesis, es considerado un factor importante en su eficiencia. Para estos propósitos, la caracterización de este material es extremadamente importante porque entre todos estas caracteristicas que podemos analizar, el número de capas va a determiner algunas propiedades principales sobre el material. Así, con el fin de identificar el número de capas de una hojuela de grafeno, es necesario aplicar dos importantes técnicas. En general, existen varios métodos de caracterización que nos pueden ayudar a completer esta tarea, sin embargo en este trabajo vamos a implementar dos de ellas. Estas ténicas son análisis de contraste óptico y espectroscopía de Raman. Although the optical contrast analysis is considered the simplest technique to determine the number of layers of 2D materials, it is very easy to use due to the employment of free software (ImageJ) accompanied with good results. Aunque el análisis de contraste óptico es considerado la técnica más sencilla para determinar el número de capas de materiales bidimensionales, es muy fácil de emplear debido a el uso de un software de libre acceso llamado ImageJ y acompañado de resultados precisos. Por otra parte, la espectroscopía de Raman podría ser complicado de implementar porque es difícil de diferenciar entre dos o mas capas presentes en el material y requiere equipo de laboratorio complejo. A pesar de eso, la espectroscopía de Raman será utilizada en este trabajo para complementar los resultados obtenidos del análisis de contraste óptico. El principal objetivo de este trabajo es ser capaz de identificar el número de capas usando el método de análisis de contraste óptico y que pueda ser reproducible en cualquier computadora debido al software de libre acceso que empleamos aquí. Por lo tanto, este trabajo contribuirá en la determinación de número de capas para cualquier material bidimensional hacienda el uso de este simple método presentado aquí.

Palabra clave: Electrónica, Espectroscopía, Bidimensinal , ImageJ, Substrato.

Contents

List of Figures

List of Tables

Chapter 1

Introduction

Graphene is a relatively new material with a lot of applications in many fields. The efforts of scientists to find a way to synthesize this material at an industrial scale are increasing day after day. The characterization of this material is an important feature that can be achieved through numerous techniques. The quantification and determination of the intrinsic properties of graphene are very essential due to the variation of these properties according to the thickness and shape of graphene. Why is a big part of the scientific community looking for obtaining graphene in bigger quantities? Which are the properties that make graphene a very useful material for some applications? What are the advantages of certain characterization techniques among others? This research aims to the optimization of the synthesis of graphene by employing the mechanical exfoliation technique. Additionally, the identification of the number of layers present in a sample of graphene is going to be elaborated. Then, we are going to answer these questions through the next pages of this work.

First and foremost, the characterization and determination of the thickness of graphene by employing two different techniques are performed and studied in this work. A wide introduction mostly related to the structure, properties, and applications of graphene will be given in the first chapter. Moreover, the theoretical background associated with the properties and applications of the characterization methods to analyze graphene will be given in context at the end of this chapter. To summarize, we are going to determine the number of layers of graphene by employing an optical contrast analysis. Then, the motivation and importance of this research work, including the main objectives, will be stated in the second chapter. Consequently, the methodology that makes this work reproducible will be presented in chapter 3. The characterization techniques and their basic principles are going to be in this chapter as well.

1.1   Carbon-Based Materials: Carbon Allotropes (0D, 1D, 2D, 3D)

Carbon is the most important element studied by human being. Denoted with the letter "C", carbon is present in many systems and processes performed on Earth due to amazing chemical flexibility, and the ability to bond with a wide variety of elements. Studies over carbon revealed that it has a versatile behavior with oxidation numbers between -4 and 4+, where it can act as a cation, as an anion, and as a neutral species.[1] Moreover, carbon possesses the capacity to

bond to itself leading to the existence of carbon allotropes. First and foremost, it is crucial to know that an allotrope is the same chemical element except that has a distinct structure. [2] The carbon allotropes are diamond, graphite, and fullerenes, which include carbon nanotubes. Furthermore, the structural arrangement of carbon-based materials is ruled by the type of hybridization. In general, hybridization is a binding between molecular orbitals, which depend on the sign of the orbital, in an antibonding and bonding structure [3]. Hence, two important hybridizations are shown in figure 1.1. Basically, the electronic configuration of a carbon atom is given in the following way: $[He]2s^22p^2$. This configuration allows the ability of carbon to bind two additional molecules. However, the energy difference between 2s-state and 2p-state is small, so that one electron from the 2s-state can be excited into a 2p-state. In figure 1.1a we can appreciate the four hybrid orbitals in sp^3 hybridization, which are conformed by one s-orbital (s) and three p-orbitals (p_x, p_y, p_z) resulting from the excitation of the electron from the 2s-state. This combination of the four hybrid orbitals form a tetrahedral assembly with a characteristic angle among all the orbitals of 109.5 degree and is observed in figure 1.1a. The structure of diamond is resulting from the sp^3 hybridization of the carbon atoms, which is going to be described in detail in the next sections.

On the other hand, there are only three hybrid orbitals in sp^2 hybridization. Here, one s-orbital (s) is combined with two p-orbitals (p_x, p_y) forming a planar assembly with a characteristic angle of 120 degrees between the hybrid orbitals, where σ-bonds are present. This scheme is represented in figure 1.1b. Additionally, there is a p_z orbital perpendicularly to the hybrid orbitals forming a π-bonds. Graphite and graphene are an example of this hybridization. In graphene, the carbon atoms are connected by the sp^2-hybrid orbitals producing a layer of graphene. Furthermore, the π-bonds give rise to weak Van der Waals forces between more layers of graphene forming the structure of graphite [3].
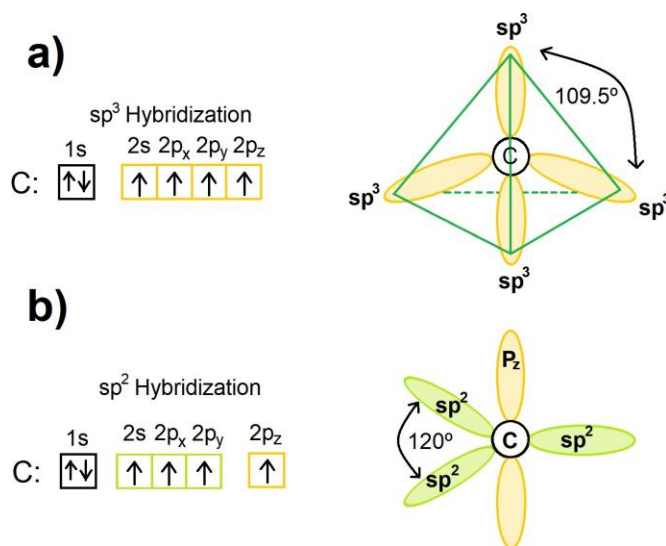
Figure 1.1: Two different types of hybridization present in carbon. a) showing the sp^3 hybridization and b) the sp^2 hybridization of carbon.

Nowadays, the incredible properties of carbon-based materials have motivated scientists to concentrate on their study and development around the world. This revolutionary element in its different forms has brought many advances in quite a lot of industries and research fields. Some famous materials are derived from carbon, such as the case of carbon nanotubes. Carbon has some allotropes that are being studied and explored due to its unique properties. Graphene is indeed the essential structure of the carbon allotropes, therefore it is the most investigated after fullerenes since its first synthesis in 2004 by Novoselov, Geim, and co-workers [4]. In addition, the physical arrangement of graphene is the one that determines the type of carbon allotrope. For example, it is been observed that the simplest single-wall carbon nanotubes are enrolled sheets of graphene. Moreover, the dimensionality determines the different carbon allotropes, which determine its basic structure and varies from 0D to 3D. [5] In general, the dimensionality of any material dictates the degrees of freedom in the system. We may observe the representation of the different allotropes of carbon in figure 1.2. Therefore, we will describe with more detail the different carbon allotropes according to their structure.
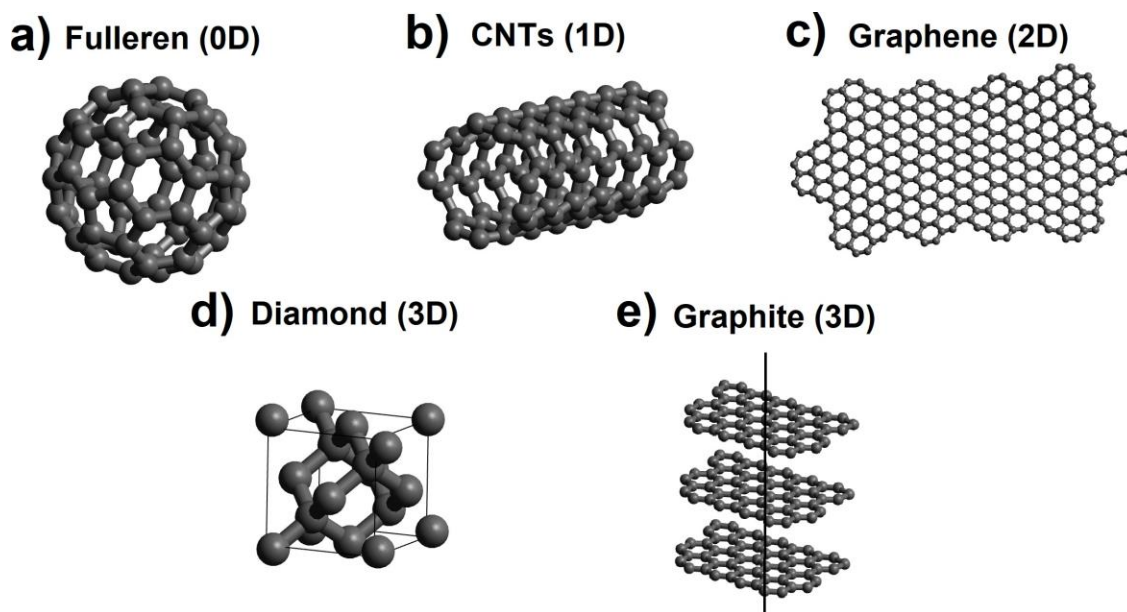
Figure 1.2: Basal structures of the carbon allotropes.

1.1.1 Fullerenes

The Buckminsterfullerene (C_{60}), or fullerene, is the most studied and investigated carbon allotrope since its discovery in 1985 by Kroto et al. of the UK. [6] This is owing to two main factors, it is attractive chemical and physical properties, and its facility to synthesize it obtaining big quantities. C_{60} is the simplest molecule among fullerenes, that posses

a spherical π-electron surface [7], which is represented in figure 1.2a. The basic structures of C_{60} are hexagonal and pentagonal rings very similar to graphite, but with zero degrees of freedom or 0D, and present an unequal double bond. Therefore, this molecule has a few configurations entirely made of carbon atoms which stand out as a hollow sphere and ellipsoidal. [8] These carbon atoms are linked to the other three carbon atoms by a covalent bond and share three of the four available free electrons producing an sp^2 hybridization. Basically, C_{60} has a spherical closed caged shape and was synthesized by employing a supersonic laser-vaporization. In this experiment, Kroto et al. observed the mass spectrum where they noticed in the spectrum a very interesting peak at 720. Using the atomic mass of carbon they deduced a relation at that peak (720/12=60), where he obtained the name for the molecule. Additionally, there are studies based on the discovery and synthesis of other similar molecules like C_{70}, C_{76}, C_{82}, and C_{84} as well. Fullerenes can be also synthesized in an electric AC arc supplying two graphite electrodes, where temperatures reach over 4000 °C. [9] Notice that these molecules always have an even number of atoms since scientists discovered this pattern without exception. Fundamentally, fullerenes are very symmetric, exhibiting a five-fold symmetry and belonging to the group of non-planar conjugated systems. [8] C_{60} and C_{70} have the best defined spherical structure, thus they are the more stable ones. Also, both consist of 20 hexagonal and 12 pentagonal rings, with an approximated diameter of $d \approx 0.7$ nm. The Euler theorem state that a closed surface consisting of hexagons and pentagons has exactly 12 pentagons and an arbitrary number of hexagons. [10] C_{60} follows the theorem, thus the smallest fullerene available is C_{20} although the strain produced due to the incompatible geometry of two pentagons (pairs) lead to an unstable molecule.

In addition, there is an especially interesting fact in fullerenes, the pyramidalization. In this molecule exists a distortion of the geometry because of its spherical form that makes carbons to be pyramidalized. This distortion leads the molecule to a tetrahedral geometry obtaining new chemical properties like a distinctive reactivity. [11] The equation given by $\vartheta p = \vartheta \sigma x - 90$, describes the pyramidalization of fullerene. Furthermore, exist a rehybridization process that suggests a change in the hybridization from sp^2 to sp, involving the inclusion of a p orbital and provoking a shift to trigonal planarity. [11] Also, C_{60} is considered an electronegative material because of the presence of empty low-lying π orbitals that behave as s orbitals. The high electronegativity of C_{60} makes them a very valuable materialfor the building of photodiodes, which was expected to create complex charge transfers with conjugated polymers. [7]

1.1.2   Carbon Nanotubes

The simplest idea of Carbon nanotubes (CNTs) is described as a layer of graphene wrapped up until achieve the form of a one-dimensional cylindrical tube. This basic structure is represented in figure 1.2b. Also exists a wide variety of designs of CNTs depending on the arrangement of carbon atoms, or the graphene layer. For instance, the number of enrolled graphene layers changes the composition of the CNTs, leading us to obtain single-walled CNTs (SWCNTs) and multi-walled CNTs (MWCNTs). [12] This construction is not that simple since, to obtain the properties that CNTs provide, two equivalent sites of the hexagonal lattice of graphene must coincide. Particularly, CNTs can be considered as elongated fullerenes, with an approximated range of diameter between 1nm and 70 nm, and a length that falls in the micrometer range. [9] Although their structural base is a graphene layer, they differ from the electric properties of other carbon allotropes due to the diversity of structural shapes. These numerous forms and shapes that

CNTs can take, even the number of layers, lead them to behave like metals or semiconductors. The special properties of CNTs are subjected to the circumference that can be expressed in its chiral vector:

$$C_h = na_1 + ma_2 \qquad (1.1)$$

Where m and n are integers corresponding to the vectors as shown in figure 1.3, and a_1, a_2 are the primitive lattice vectors represented by n and m. Additionally, ϑ must be introduced as the angle between the chiral vector C_h and the zig-zag direction and is defined as:

$$\vartheta = arctan \left(\frac{\sqrt{3}n}{2m + n} \right) \qquad (1.2)$$

In principle, The value of the angle determines the direction of the arrangement of the CNT. Three types of CNTs can be obtained, zig-zag, armchair and chiral CNTs with angles of $\vartheta = 0$, $\vartheta = 30°$ and $0 < \vartheta < 30°$, respectively. It should be noted that the types of CNTs also depend on the values of m and n. Hence, these types can be identified by the values of n and m in table 1.1.

CNT	Indices (n,m)	Chiral vector
Zig-zag	(n,0)	0°
Armchair	(n,n)	30°
Chiral	(n,m), m≠0	$0 < \vartheta < 30°$

Table 1.1: Type of CNT according to its n, m indices. This table was elaborated based on the studied performed by Eatemadi *et al.* [13].

The diameter of the CNT is expressed in the following way:

$$d = \frac{a\sqrt{m^2 + mn + n^2}}{\pi} \qquad (1.3)$$

Where a is the lattice constant which is given by $a = 1.42 \times \sqrt{3}$ Å for the reason that for sp^2 hybridization (graphene), the C-C bond distance is 1.42 Å. The representation of the different types of CNTs is shown in figure 1.3. Here, the yellow line follows a zig-zag pattern, while the red line follows the armchair pattern. Additionally, we can construct a chiral CNT by following equation (1.1) which is also represented in figure 1.3.

The synthesis of CNTs basically involves a carbon source, a metal catalyst, and heat. [14] Therefore, CNTs can be synthesized by arc discharge between two graphite electrodes, laser evaporation of carbon, and chemical vapor deposition (CVD). CVD is a very known technique by the scientific community, and not only to synthesize carbon materials. The three methods present a good efficiency to produce high-quality CNTs. However, CVD provides the option of large-scale production of CNTs, which is a big advantage speaking in industrial terms. [15] This method can also synthesize other types of carbon fibers and MWCNTs with the same efficiency, and high-quality. [16] Another advantage offered by this method is the allowing of the CNTs to be previously defined for a specific area. For example, the growth of CNTs on certain substrates can provide a route to the use of CNTs in the field of electronics.
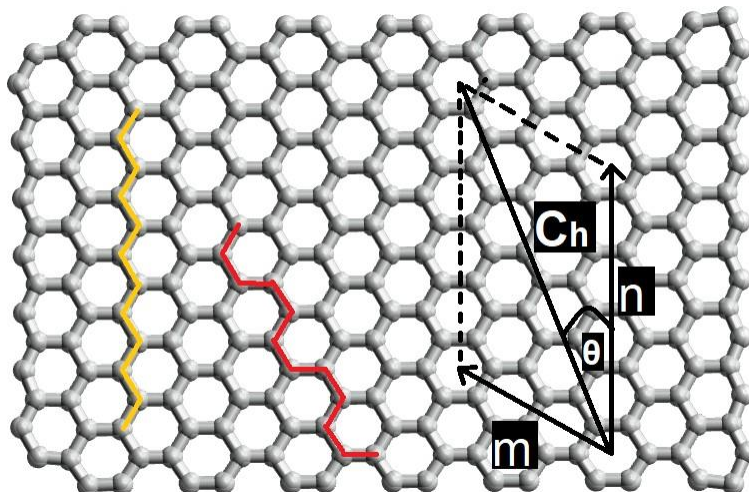
Figure 1.3: Representation of CNTs (5,3) with different n,m indices.

CNTs have attracted the attention of many researchers due to their multiple amazing properties, such as mechanical and electrical properties. As an example, recent studies show that CNTs have demonstrated a high strength and stiffness, being capable of holding pressure of about 24 GPa remaining just after graphene as the hardest material. [17] Moreover, CNTs are tremendously conductors, where electron wavevectors are quantized along the tube, allowing the charge carriers to move freely in the axial direction. [18] Besides, it is amazing that CNTs can behave as a semiconductor or metal-based on m, and n values. Then, CNTs can behave as quantum wires and making them more functional than conventional wires and having a wide range of applications in electronics. [19]

1.1.3   Diamond

Another carbon allotrope is the diamond, which is contemplated as a natural 3D crystalline structure of pure carbon. The carbon atoms conforming diamond present an sp^3 hybridization, forming a regular tetrahedron. This assembly is shown in figure 1.2d. Subsequently, the bond length in sp^3 is around 1.56 Å. In this structure exists four bonds pointing directly to each corner of this tetrahedron, establishing a three-dimensional arrangement of carbon atoms characterized for being extraordinarily hard. [20] In comparison with graphite, diamonds behave as an insulator because of the localization of the electrons in an sp^3 hybridization, which forms σ bonds. Besides, diamond owns a high elastic modulus, hardness, and thermal conductivity at room temperature. This is explained because of its low thermal expansion coefficient and elevated optical band gap. [21] In this crystal, the σ bonds stay at negative energies and give a resultant valence band filled with bonding states (σ), which leads to obtaining a high band gap since the conduction band is empty. [22] The approximated 5.5 eV band gap should explain the low conductivity observed in this

crystal.

Furthermore, exists other types of crystallographic compounds often known as diamond-like phases, which can be synthesized in a laboratory. Afterward, pressure, temperature, source material, and medium composition are some conditions that guide its formation and synthesis. As a matter of fact, it has some interesting properties as mechanical and exorbitant anti-corrosion features. Nevertheless, this material is limited by the excessive cost of synthesis. [23]

1.1.4   Graphite

Graphite has been studied since many years ago by many scientists that observed its unique properties. Among them, stand out the electric and thermal conductivity. Firstly, graphite is anisotropic with a trigonal sp^2 hybridization differing from diamond. For this reason, graphite consists of carbon layers pilled up one on top of each other forming a 3D structure with an interplanar distance of about 2.7 times greater than C-C bonding and stacking in an AB sequence (different from HCP stacking). [24] A basic representation can be observed in figure 1.2e. These carbon layers, or graphene, are bonded by weak van der Waals forces. In this configuration, the electric conductivity will be more efficient within layers than perpendicularly due to the van der Waals forces. The anisotropy observed in graphite makes it chemically reactive, in which reactants are able to remain between layers. This process is often known as graphite intercalation compound (GIC) and gives way to the formation of other compounds. This intercalated compound improves significantly the electric conduction between layers. [25]

Usually, impurities present in the crystal avoid the study and analysis with great precision. Therefore, the implementation high oriented pyrolytic graphite (HOPG) increases the accuracy of the measurements. In other words, HOPG is a similar graphite crystal but with the axis well aligned. Research done shows that the reflectance spectrum of HOPG is almost identical to natural graphite crystals. [26]

Natural Graphite crystals by themselves suffer a lack of applications. However, GICs have a broad range of applications due to their increased conductivity in comparison with graphite. Thus, new studies have been made related to the intercalates between graphene layers. For example, with the purpose of increasing the conductivity, different families of intercalates have been tested of which we can highlight pentafluorides, metal chlorides, fluorine, alkali metals, and halogens. [27] Certainly, graphite and graphene share similar properties due to the fact that they are coupled between them. As an example, we may observe that both possess the same sp^2 hybridization, which makes graphite and graphene have equivalent electric behavior. Hence, we are going to describe the electric properties of both below.

1.2   Graphene

Graphene is a relatively new material synthesized for the first time by Novoselov and Geim and explored by many researchers due to its amazing electrical, mechanical and optical properties. Initially, it is important to state the molecular structure of carbon in order to understand the properties of graphene. One carbon atom has four valence electrons prepared to form bonds with other atoms, therefore in graphene exists C-C bonding forming three σ and one

π bonds. This is called sp^2 hybridization and it allows graphene to have applications in electronics [28]. Additionally, the structure can be observed in figure 1.2c. The base structure of graphene is a single layer of carbon atoms arranged in a two-dimensional hexagonal honeycomb lattice with a bond length of 1.42 Å.

Back then in 2004 when Geim and Novoselov described and reported highly innovative experiments of graphene. The scientific community started to observe with attention these experiments, especially the physics community. It was not until 2010 that Geim and Novoselov won the Nobel prize in physics because of the paper presented in 2004. Among the many features of this paper, the most important is the sample preparation used to obtain high-quality monolayer and few-layer graphene flakes. This is a simple technique based on the mechanical exfoliation of graphite that can be easily replicated by anyone. In addition, they reported a linear dispersion relation $E(k)$ for electrons and holes mostly related to massless Dirac fermions [29].
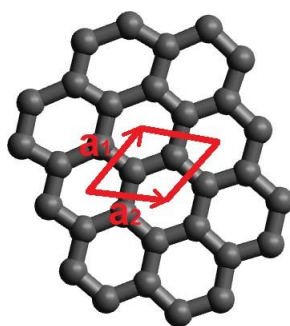
Figure 1.4: Unit cell of graphene.

1.2.1   Properties of Graphene

The unusual properties of graphene have made it an interesting material for scientists. These properties take advantage of other materials in many fields, especially when working with monolayer and few-layer graphene. In particular, graphene has an ultra-high intrinsic carrier mobility of $2\text{x}10^5$ cm$^2 \cdot$ V$^{-1} \cdot$ s^{-1}, a higher surface than single-wall carbon nanotubes reaching 2630 m$^2 \cdot$ g^{-1}, and high thermal conductivity overtaking the values for copper. All these properties make graphene a valuable material with excellent mechanical, elastic, and thermal properties [2]. Besides, graphene possesses exceptional charge transfer, optical and band structure properties, making it tremendously functional in many scientific and technological fields. We can find these amazing materials in recent electronic works, where they can fit perfectly due to their unique electronic and optical properties. In addition, graphene-based materials share their properties having a big impact on electronic devices and photo-electronic devices such as circuits, sensors, and energy storage devices. According to Prof. Jiri Minaret "Graphene can explore many novel uses in a variety of fields including transparent and flexible electronics, and electronics that are greatly quicker than existing one, and even beyond its digital applications, for example, the addition of graphene powder in tires make them stronger." [30] Additionally, graphene cannot be enclosed in one material since it can be functionalized

and be added to other materials such as many types of plastics with the purpose of forming hybrid materials. The most important properties of graphene are described below:

- It has a high specific area of about 2630 $m^2 \cdot g^{-1}$.

- Its intrinsic mobility mentioned before about $2x10^5$ $cm^2 \cdot V^{-1} \cdot s^{-1}$.

- It has a big Young's modulus about 0.5 TPa.

- It has a thermal conductivity of 5000 $W \cdot m^{-1} \cdot K^{-1}$.

Moreover, graphene presents an optical transmittance of approximately 98% with a zero band gap and outstanding elasticity. Also, nowadays it is known as the lightest and thinnest material. Additionally, graphene is ready to be chemically functionalized, allowing it to be used in liquid or dry states[31].

Electronic Properties of Graphene

One important characteristic of graphene is the zero band gap that converts it into a material with high electrical conductivity. As described before, one carbon atom has four valence electrons ready to be bonded. However, three of four electrons are used to form bonding between carbon atoms in the sheet of graphene. This configuration that leaves one free electron is responsible for the formation of π bonds giving graphene an exceptional electronic conduction. Since these electrons are located above and below graphene, the electronic properties depend exclusively on bonding molecular orbitals and anti-bonding molecular orbitals of π electrons. It is very important to mention that the electrons and holes, also called Dirac fermions, present in graphene have zero effective mass due to the presence of six individual corners of the Brillouin zone, or Dirac points, in graphene. For this reason, electrons in graphene can easily be represented as photons that can move extremely fast owing to the fact that they are almost massless. We can observe this phenomenon according to the intrinsic mobility reviewed above. Besides, graphene can be doped to increase the conductivity even more than any other material at standard temperature and pressure. The conductivity mentioned can be known as ballistic transport as stated by quantum mechanics including the fact that electrons do not present scattering.[32]

Optical Properties of Graphene

As seen before, electrons in graphene act as photons in a certain way. This phenomenon affects the optical properties of graphene making it to absorb a significant fraction of about 2.3% of white light. Additionally, the peculiar structure of graphene affects this absorption of white light. This quantity is truly related to a single layer of graphene. If we add another layer of graphene, the light absorbed will increase about the same fraction of 2.3%.[33] Apart from this, graphene is capable to absorb photons from the visible to the infrared range and has the highest strength of the interband transition.[34] Recent studies have shown the transmittance spectra and the dynamical conductivity of graphene, which is related to the optical properties. The dynamical conductivity was found to be $\sigma(\omega)=e^2/4k$. When compared to the dynamical conductivity, instead of the spatial dispersion of conductivity, over the visible frequency

range, the graphene's opacity is approximately $\pi\alpha \approx 2.3\%$. [35] This feature leads to a saturable absorption when the optical intensity reaches some specific threshold.

Mechanical Properties of Graphene

Another important feature of graphene is its massive strength, being known as the strongest material in the world. Additionally, graphene presents a weight of 0.77 mg/m^2, which is extraordinary light. Studies show that we can take advantage of this property to synthesize 3D interconnected graphene networks to obtain a lightweight material of about 2 mg/cm^3. [36] In order to understand why is this feature present, we need to observe graphene at the atomic scale. Basically, the 1.42 Å C=C bond is responsible for the strength, this characteristic is the one that makes the tensile strength of graphene to be described in Gigapascals. [37] As mentioned before, graphene has a large Young's modulus, but it also possesses a range of spring constants depending on the region of about 1 N/m to 5 N/m. These characteristics and the employ of an atomic force microscope made the scientists state that one single pure graphene sheet is capable to support the load of an elephant. [37] These properties with the combination of the electrical and optical properties make graphene a very "magical" material that easily can improve many materials used currently.

Thermal Properties of Graphene

The thermal properties of graphene play also an important role in its applications. We have already said the thermal conductivity of graphene, which is $5000 \ W \cdot m^{-1} \cdot K^{-1}$ and stands out since it is the highest of the other carbon allotropes. Firstly, in order to completely understand its thermal properties, we should go through the lattice vibration modes or phonons and the specific heat of graphene, and analyze its unit cell. As shown in figure 1.4, graphene has 2 carbon atoms per unit cell, which establishes three acoustic and three optical modes. [38] Although, the specific heat of graphene is not available, exists experimental data for graphite. In general, phonons and free electrons store the specific heat given by $C = C_p + C_c$. Besides, when working at all feasible temperatures, the phonons are in charge of the specific heat of graphene. As well as that, exist an increment of the phonon-specific heat with temperature. The specific heat of graphite is approximate $C_p \approx 0.7 \ J \cdot g^{-1} \cdot K^{-1}$ at room temperature, which is around a third part of the classical upper limit. [39] Particularly, if we compare the specific heat between graphite and diamond, we can appreciate that, at room temperature for graphite, this value is approximately 30% higher than for diamond. This difference is mainly due to a not so strong coupling between graphite layers. Therefore, we can deduce that in graphite exists a higher density of states at low phonon frequencies. [39] Thus, for an isolated graphene layer, is to be expected an akin behavior of course, at room temperature.

1.2.2   Synthesis of Graphene

Currently, exists numerous and complex techniques to synthesize graphene. Few of these techniques are more complex than others, varying between the equipment used and substrates if they are employed. Some of these methods are known as chemical exfoliation. However, graphene can also be obtained by mechanical exfoliation, which is a simpler technique. In addition, exist other types of techniques that are CVD, PVD, by reduction of

graphene oxide, and electrochemical expansion. All types of methods have their advantages and disadvantages. For example, synthesizing graphene by applying a chemical exfoliation presents tedious, time-consuming, involves the use of highly hazardous chemicals which creates severe environmental problems, and the obtained graphene can present defects [19]. Although mechanical exfoliation methods can lead to the obtaining of high-quality graphene, the performance of this method is poor and highly time-consuming. The more efficient method to synthesize graphene is chemical vapor deposition (CVD), with an obtaining of highly pure graphene. However, this is a highly cost method that requires special equipment, which cannot be easily found in an ordinary laboratory. Furthermore, in the electrochemical expansion method, we are able to obtain pure graphene with a time-efficient as well. Unlike CVD, this method is low-cost and is used to produce high quantities of graphene. In general, the scientific community is looking for new cheap-cost methods in order to produce single-layer graphene and few-layer graphene. However, in this work, we are going to present in detail the synthesis of graphene by mechanical exfoliation.

Graphene Synthesis by Micromechanical Cleavage

The micromechanical cleavage was the first technique employed to obtain graphene flakes from graphite. In principle, we can peel off graphene from any natural graphite, however, we can implement high oriented pyrolitic graphite to this technique to improve the quality of graphene flakes. Also, the crystals of graphene peeled off can have lengths on the order of micrometers. HOPG is synthetic graphite formed by cracking a hydrocarbon at high temperatures and subsequent heat treatment, often combined with the application of pressure. [40] Novoselov et al. carried out this technique in 2004, where they obtained and studied single-layer and few-layer graphene. [41] Nevertheless, this technique normally leads us to obtain bilayer graphene with an AB stacking arrangement. Therefore, the atoms per unit cell in bilayer graphene, which is four atoms, is the same as for graphite. [42] The repetitive use of this technique, usually known as the scotch tape method, is also a highly practical technique to obtain other atomically flat crystals. Therefore, many specialists in scanning probes have been using this technique many years ago and obtaining nice samples to analyze in the atomic force microscope and scanning tunneling microscope. Then, this technique itself is not innovative and worthy of a Nobel prize as numerous people think. What Novoselov et al. reported was that applying this technique multiple times can lead us to obtain thinner flakes even single-layer and bi-layer graphene. As a consequence, they could perform the necessary experiments and report many unique important, and amazing aspects of graphene-like the quantum hall effect. This method has one big advantage, the process and the equipment are not difficult to obtain. Hence, the basic principle of this method is to adhere a piece of scotch tape onto graphite and peel it off the surface as observed in figure 1.5. In this way, graphite flakes are going to be stuck to the piece of tape. By adhering another piece of tape onto the one with graphite flakes and repeating the process several times, we are going to be able to obtain thin layers of graphene. This technique allows us to break the van der Waals forces that maintain the graphene layers attached perpendicularly between them. [40] Then, this process can be repeated as many times as desired to obtain thinner and thinner layers, even thinner until we reach with few-layer graphene. Once we obtain the flakes in the tape, we transfer them to any substrate. The most common substrate used is SiO_2 on silicon because the graphene layer can attach to the substrate without effort by simple electrostatic interaction. Following these basic steps, we can have graphene layers, however, the important thing to accomplish is the characterization of the sample in order to realize how many layers of graphene exist in the sample. We can achieve this with numerous

characterization techniques, although the most common and easy to use is an optical microscope where we can dispose of a lot of time characterizing the sample.

From the procedure described above, we can observe advantages and disadvantages. On one hand, the method and the equipment used to develop the synthesis is easy to manipulate and obtain. In addition, we are able to isolate the large area and high-quality flakes. On the other hand, this is a highly time-consuming technique with a low efficiency speaking on the quantity of graphene produced, and it can hardly be used for industrial production. Besides, the amount of polymer corresponding to the tape present in the substrate is elevated, and a post-heat treatment is required.[43] Evidently, this technique is also employed a lot for demonstrational and educational purposes.

Figure 1.5: Synthesis of graphene by mechanical cleavage of HOPG.

In figure 1.5, we can appreciate the corresponding process to obtain graphene layers. Here, the exfoliation of the graphite with the help of the scotch tape is shown to later move the layers to the Si substrates, which are the squares inside the Petri dish.

1.2.3 Applications of Graphene

Since its discovery, graphene and derivatives have been studied and classified for a wide range of applications in many fields. Its principal applications remain in some important areas such as nanosensors, nanocomposite materials, nanocatalysis, nanoelectronics, nanobiotechnology, and bioenergy due to its very unusual properties. The field of nanoelectronics received with open arms graphene owing to the fact that its electronic properties enable graphene to be used in brand new electronic gadgets.[44] Therefore a lot of research is carried out, even for big companies, in the field of nanoelectronics. Fundamentally, nanoelectronics is the incorporation of nanotechnology into plenty of electronic systems. Additionally, if we implement graphene to this concept, the possible developed electronic components could achieve extraordinary properties principally due to the zero band gap, high surface area, and high electron mobility. Furthermore, edge planes of graphene provide high-efficiency electrocatalytic properties towards redox electrolytes.[45] Subsequently, these characteristics make graphene be used as a counter electrode material employed a lot for dye-sensitized solar cells. Usually, graphene electrodes are coated with a polymeric binder on conducting substrates.[46]

Nevertheless, not only electronic properties of graphene make it practical, but also optical properties offer big advantages. Such is the case of mode-locking of fiber lasers which are ultrafast fiber lasers that can be actively or passively mode-locked, it enables the generation of ultrashort pulses. [47] We can achieve a full band mode-locking utilizing an erbium-doped dissipative solution fiber lase. This procedure allows obtaining a 30 nm wavelength tunning because of the wavelength insensitive ultrafast saturable absorption of graphene. [19] Similarly, graphene is used as a photodetector based on the fields created at the metal contacts of graphene. In recent studies, visible and infrared light was irradiated to segments, of about 200 nm, of graphene that was brought in contact with palladium. Then, it showed an AC photoresponse of a single junction detector to a modulated light beam of 1.55 μm. [4]

The characterization of the graphene flakes is an important process as well. It can help us to determine some properties and defects of the samples. For our specific case, we are interested in determine the thickness i.e. the number of layers of graphene. Generally, exist a few methods, including spectroscopic techniques, to identify the number of layers. Not withstand, the optical contrast method may help us to obtain the number of layers without difficult, and it is going to be described next.

1.3 Determination of Number of Layers of Two-Dimensional Sheets

Currently, the study and characterization of two-dimensional materials are attracting the attention of the scientific community. The principal reason lies in the variations of their physical and chemical properties with respect to bulk crystals. [48] Essentially, the best method to obtain high-quality nanosheets is mechanical exfoliation. This method is described in detail for the obtaining of single and few-layer graphene in the previous section. Although with this method we acquire high-quality nanosheets, we are not able to control their thickness with precision. It is fundamental to have information on the thickness of a 2D nanomaterial since some of its properties vary according to its thickness. As a result, the applications of the nanomaterial are affected by the thickness of the nanosheet. This is the principal reason to find the best method to characterize the thickness of our 2D nanosheet.

As a matter of fact, there are three techniques that lend a hand to us so that we can appreciate the number of layers present in a certain sample. These methods are atomic force microscopy (AFM), Raman spectroscopy, and optical microscopy. For our specific case of graphene flakes, we can use any of these techniques, but AFM is well-known to be time-consuming for analysis over a large area of a material. Some issues present in the equipment and the absorbed water under the samples are other disadvantages of this method as well [49]. Hence, we are going to review the two more important techniques to identify the number of layers of graphene, optical microscopy, and Raman spectroscopy.

1.3.1 Optical Contrast Analysis

On the other hand, optical microscopy is considered an uncomplicated and quick technique to determine the thickness of, not only graphene but also 2D nanosheets over a large area [50]. The main feature of this method is based on the optical contrast present in any observable image. Evidently, the better the optical contrast of the image, the better and more precise results will be obtained. Hence, this optical contrast is based on the contrast difference produced
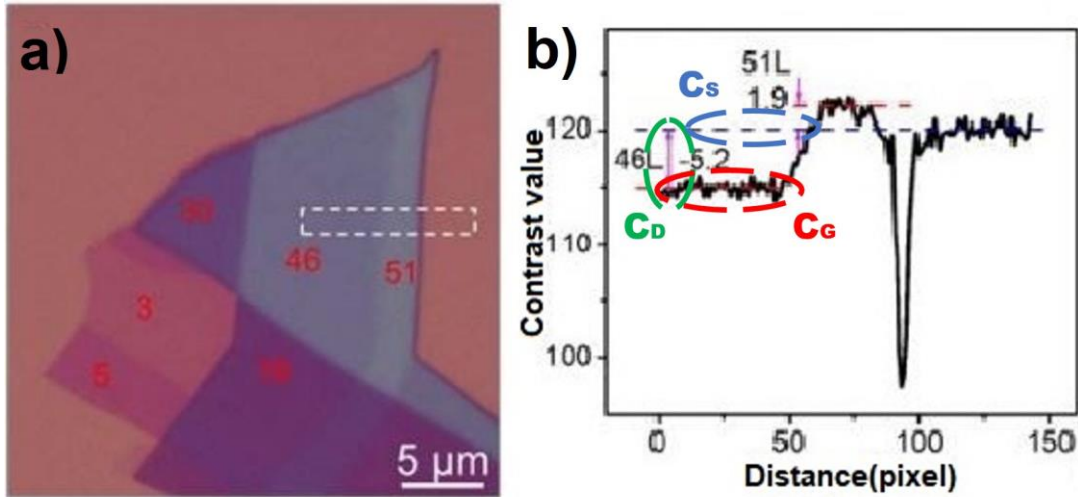
Figure 1.6: a) Optical contrast analysis performed on a graphene sample showing the optical path and b) the contrast profile. Image retrieved and modified from Li *et al.* [48].

by the graphene with respect to the substrate. Therefore, it is very important to be able to observe and obtain the contrast values of the substrate. The main basis of this interaction relies upon the fact that each layer of graphene absorbs a certain portion of the light emitted onto the nanosheet. The theoretical principles of this effect will be explained later. In addition, image processing is exceptionally important for this technique because we require to enhance the optical contrast of the sample images. Even though the values of thickness observed from this method are more exact and easier to obtain, is necessary to possess the knowledge of image processing to acquire reliable data.

The contrast difference between the sample and the substrate is the key to determine the number of layers of the nanosheets. Hence, by subtracting the contrast of the sample with the contrast of the substrate, we can obtain the contrast difference values, which is given in the following way:

$$C_D = C_G - C_S \tag{1.4}$$

Where C_D is the contrast difference value, C_G is the optical contrast of the graphene sample, and C_S is the optical contrast of the substrate. This process is closely related to the manipulation of the ImageJ software, which is also going to be employed in this work. This software allows us to obtain the initial gray values that will help us to calculate the contrast difference values, as observed in equation (1.4).

In figure 1.6a, we can observe an optical image of a graphene sample showing a section with multiple layers, where the rectangular square represents the area to analyze. The contrast profile, where the information of the number of layers remains, is shown in figure 1.6b. This graph is always representing the contrast values of the dotted

square, observed in the graphene sample in figure 1.6a, from left to right. Therefore, we observe we start with the contrast of 46 layers. After that, the curve increases the contrast values of 51 layers. Although we took 46 layers as the reference for C_G, this value could be taken as the contrast of 51 layers. Finally, it ends with the contrast values of the substrate represented as C_S. The pronounced valley shown in the figure is due to the contrast value of the edge of the graphene sample, which seems to be of a lower number of layers since it appears to be darker than the other regions shown. From this figure, we can obtain the contrast difference values using equation (1.4). The representation is shown in the figure, where the C_D is obtained by subtracting the C_S from the C_G. Thus, these contrast values are later compared with theoretical values in order to determine the number of layers present in the graphene sample.

1.3.2 Raman Spectroscopy Analysis

Raman spectroscopy technique, which can also help us to identify the number of layers of graphene, results in a better and quicker characterization than AFM in terms of the low number of layers of the 2D nanomaterial. Despite the fact that we can identify with ease monolayer and bilayer nanosheets, the results between double layer and few-layer nanosheets are hard to differentiate. This technique is based on the Rayleigh scattering and is going to be described in detail in the following sections. Here, we are able to identify the nature of the material because there are specific peaks for a certain material. In our case, graphene is outstanding to present 3 main peaks. The peak located at approximately 2700 cm^{-1} is the one that gives us information related to the thickness of graphene.
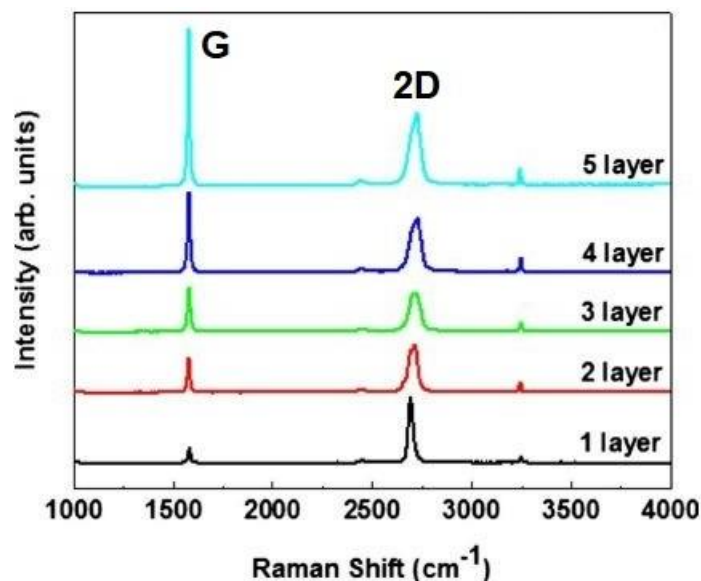
Figure 1.7: Raman spectra of graphene of different thickness or number of layers. Image retrieved and modified from Calizo *et al.* [51].

As observed in figure 1.7, Calizo *et al.* [51] performed a Raman analysis over graphene with a different number of layers. Initially, for monolayer graphene, we can observe that the peak corresponding to the 2D band is narrow with a notable peak. In this form, we can identify monolayer graphene without effort, however, we present some difficulties in differentiating the peak between bilayer graphene from graphene with 3 or more layers. This issue is mainly due to the fact that the Raman spectra for two or more layers of graphene are very similar and the identification of the number of layers is not so trivial. This feature is observed in figure 1.7, where we can appreciate a clear difference between the main peak (2700 cm^{-1}) of one layer and two layers of graphene. On the contrary, it seems to be difficult to state a difference among the Raman spectra of two or more layers of graphene.

Chapter 2

Motivation

There exists numerous methods to produce graphene flakes, nevertheless the properties of graphene may differ depending on the method employed to produce it, which is related with the number of layers in the 2D material. Hence, it is necessary to perform a characterization of the material to determine the number of layers present in the sample. Therefore, our main goal of this work is based on the presentation of a simple and reliable method to quantify the number of layers of graphene using an optical contrast method. This technique, which supports the use of an optical microscope, is considered the simplest way to determine the number of layers. The main reason is due to the interaction of light with graphene, which is absorbed leaving a notable contrast difference. Practically, we need to control the thickness of the substrate due to its dependence on this technique. Therefore, a standard measure of thickness will be intended as well. Additionally, the employment of the ImageJ software will be necessary since the optical reflectivity technique can be strengthened by applying a contrast enhancement to the graphene samples.

In addition, We also want to show a characterization of the graphene flakes using Raman spectroscopy, which is based on regular Raman scattering. In other words, this method will help us to differentiate between graphene flakes, graphite, and other impurities present in the sample. This is mainly due to the interaction of graphene with light and the facility to operate the equipment. Although there is not very easy equipment to find in a regular laboratory, there is an available Raman spectroscope in the laboratory of Yachay Tech University. Then, the experiments and characterizations could be achieved in these laboratories. As an additional factor, Raman spectroscopy is not a quantification technique, which implies that we are not able to know the exact number of layers present in the graphene samples.

Moreover, an effortless method to synthesize graphene is attempted. Subsequently the graphene flakes obtained will be characterized using the methods shown above. the synthesis of graphene by mechanical exfoliation is not one of those methods and is hard to produce big amounts. Conversely, this method allows the possibility of obtaining high-quality graphene flakes. For this reason, this method is commonly employed for demonstrational and educational purposes. Likewise, the basic methodology to obtain graphene flakes presents some inconveniences that delay the educational process. In other words, an increase in the quality of graphene flakes is desired. Therefore, we proposed to describe a detailed procedure with specific materials in this work.

Chapter 3

Methodology

3.1 Synthesis of Graphene by Mechanical Exfoliation

In general, graphene flakes were obtained by exfoliating HOPG. Even though, we were required to prepare the silicon oxide wafers for the transfer of graphene. Then, in the first, place we employed four wafers which were stuck with the brilliant surface upwards into a Petri plate, cleaning the plate with ethanol before. To get started, we need to carefully exfoliate a few layers of the graphene from the HOPG with the help of the scotch tape. We must observe a small dark portion in the tape as shown in figure 3.1a. This process leads us to have multilayer graphene on the piece of tape as appreciated in 3.1b. After that, a process of sticking and peeling off must be carried out in the tape. This process was realized approximately fifty to sixty times. We can observe the result of the exfoliation in figure 3.1d. This process is tremendously important since it allows us to obtain few-layer graphene over the whole tape. Later, we cut with care the tape with the graphene flakes to place in the wafer which will adhere easily for electrostatic interaction. In the end, we obtained four samples from the same scotch tape as shown in figure 3.1e. Finally, we cover the Petri plate and save it for later characterization. The whole process to obtain high-quality graphene flakes is shown in detail in figure 3.1. Initially, this process was performed with regular scotch tape as appreciated in figure 3.1. Nevertheless, later observations exhibit that the polymer of the scotch tape were lied on the Si substrate with the graphene layers. This represents a possible issue because it difficult the visibility of the graphene samples. As a consequence, the determination of the number of layers can be delayed because of this issue.

In order to overcome this problem, we employed a different scotch tape. This tape is an acetate tape that possesses less sticky polymer. Therefore, the same process showed before was applied with the implementation of this tape. The results reveal less polymer in the graphene sample, which facilitated the visibility to be analyzed for optical microscopy and Raman spectroscopy.
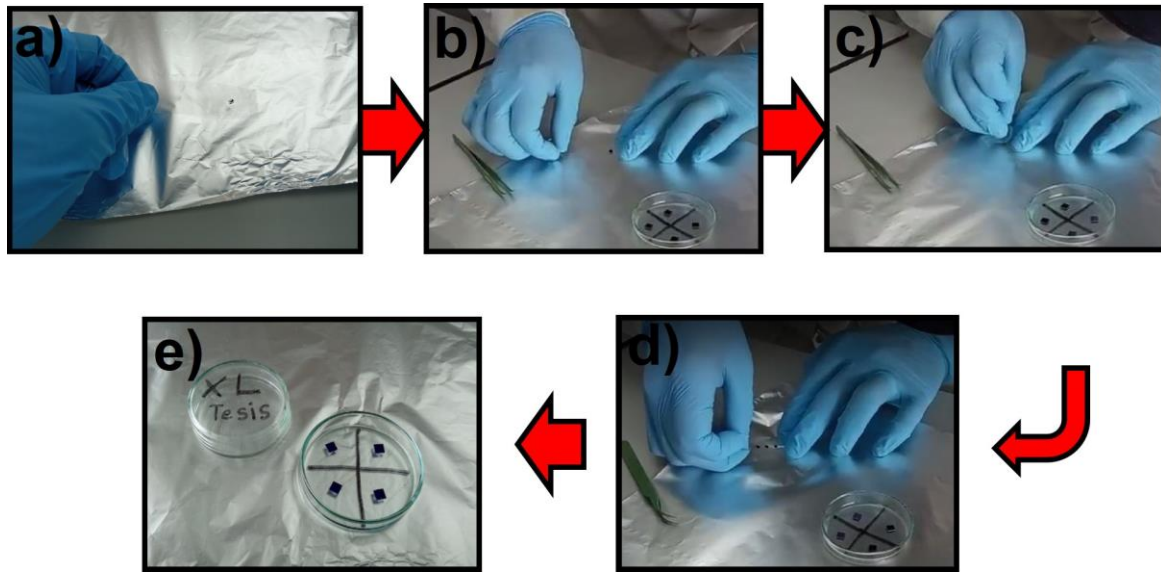
Figure 3.1: Procedure to obtain high-quality graphene flakes by mechanical cleavage. In the subfigure a, is appreciated the sample of multilayer graphene extracted from the HOPG. Next, the process of sticking and peeling off of the tape in order to separate the layers of graphene can be observed in subfigures b and c. After that, we will obtain many samples of few-layers graphene in the same tape is shown in subfigure d. Finally, the graphene samples were carried to the SiO_2 substrates in the petri plate as observed in subfigure e.

3.2 Optical Microscopy

Optical microscopy is an old technique that still has an interest in many characterization processes. This microscope allows us to work at micron and submicron levels maintaining precise results. It is used in many fields of science with many applications due to its simplicity to manipulate and analyze samples. Nowadays, this technique is able to be combined with imaging process and analysis in order to increase and quantify digital data [52]. Furthermore, the equipment is composed of an arrangement of lenses that magnifies the original image. Basically, there are two main parts of the microscope, the objective lens, and the eyepiece. The objective is closest to the sample and its principal task is to magnify the real image and project it to the eyepiece. On the other hand, the eyepiece is closest to the human eye where we can observe a virtual image produced by the objective lens. The eyepiece can be enhanced to increase the magnification of the real image as well.

A basic representation of an optical microscope is observed in figure 3.2 showing the main components of an optical microscope. Here, we have the sample, which is projected and inverted through the objective lens to the human eye. The eyepiece is fundamental because it redirects the real image to the eye forming a virtual image. Also, h and h' are the heights of the real sample and an intermediate image of the samples, respectively. The back focal length of the objective can be observed in figure 3.2 between the objective and the intermediate image.

Figure 3.2: Basic functioning of an optical microscope showing the main components. Here, we can observe how the image sample is projected and inverted through the objective lens and the eyepiece right to the human eye showing a virtual image represented as h'. This image was constructed based on Davidson and Abramowitz [52].
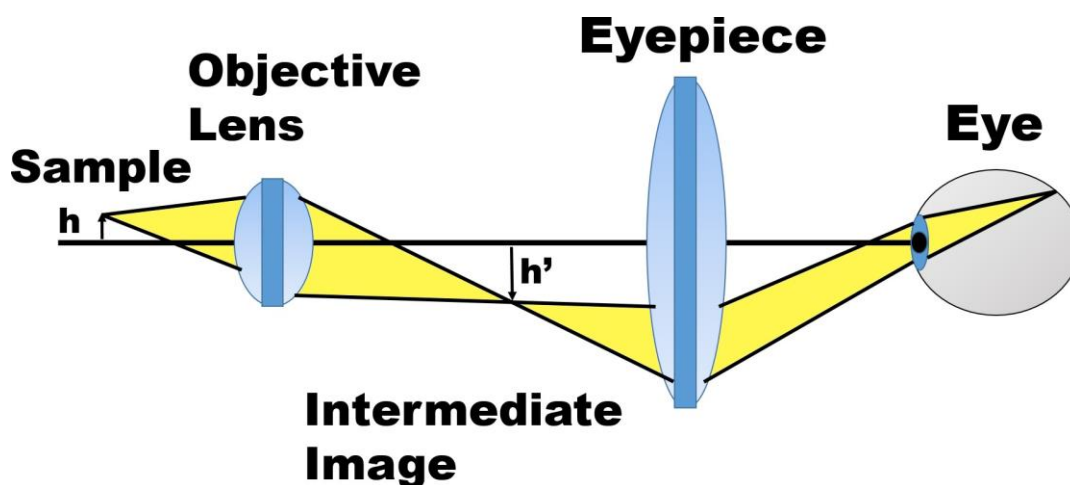
The image formation of the optical microscope is related with the light entered into the sample, which is irradiated from a lamp included in the equipment of the microscope. Therefore, light passes through the entire system, where a fraction of the light interacts with the sample and other fraction passes around the sample. As a consequence of the interaction of light with the sample, a part of this light could be absorbed by the specimen in the sample. Conversely, some fraction of the light, that is not absorbed by the sample, is reflected directly to the objective lens. This results in the formation of the image that is visualized in the eyepiece by the human eye. The light diffracted by the sample is brought to focus at various localized places on the same image plane, where the diffracted light causes destructive interference and reduces intensity resulting in more or less dark areas [52].

3.3 Characterization of Graphene using Optical Reflectivity

In recent years, many techniques to visualize and characterize graphene have been discovered. However, the employment of an optical microscope was one of the first methods to study graphene, obtained from mechanical exfoliation of course. The graphene flakes obtained from this method are thin and enough transparent to be observed in an optical path. As we mentioned before, the graphene flakes lie in a silicon wafer, thus the optical path of a graphene flake on top of this wafer will present a shift in their interference color with respect to an empty wafer. [2] The main functioning is based on the absorption of graphene, which is approximately 4%-10% of the reflected light on the substrate depending on the thickness of the SiO_2 layer. This absorption increases linearly with the number of layers until 10 layers since a 10 layer graphene can be considered as bulk graphite. For that reason, the thickness of

the SiO_2 must be taken into account to be able to observe graphene since we can contrast a single layer of graphene with this technique. In fact, a small change in the thickness of a SiO_2 (approximate 5%) would lead to a decrease in contrast. Even environmental conditions may affect dramatically the visibility of graphene. Although, we can reduce the factor of the thickness of SiO_2 with the implementation of narrow band filters. As an illustration, graphene photographs with the same conditions and taken in two different places (laboratories) offer different visibility, whose photographs were compared between Zhang *et al.* [53] and Novoselov *et al.* [41] . Likewise, the optical contrast in this technique is due not only to the optical path but also to the opacity of graphene. According to Blake *et al.* [54] graphene flakes with ten or more layers can be seen under the white light of an approximate 200 nm SiO_2. As mentioned before, if we include a narrow band filter, we are capable to observe graphene flakes with a higher thickness of SiO_2. Additionally, the contrast of graphene can differ with a shift in the wavelength λ, which implies that the visibility of graphene is affected by the color of light as well. The visibility of graphene can be affected when using different substrates due to the relative phase shift and amplitude modification induced by the graphene layer. [55] In figure 3.2a, we can observe a simple interaction of light with a single layer of graphene on a substrate, where n represents the refractive index. This is the basis of the optical analysis since it is going to determine the number of layers according to their contrast produced by this phenomena. A single layer of graphene is capable to absorb light, which influences in the contrast as well. In figure 3.3b is shown how the optical contrast is affected by the number of graphene layers, where the contrast increase with the number of layers due to the contribution of absorption and phase modification.
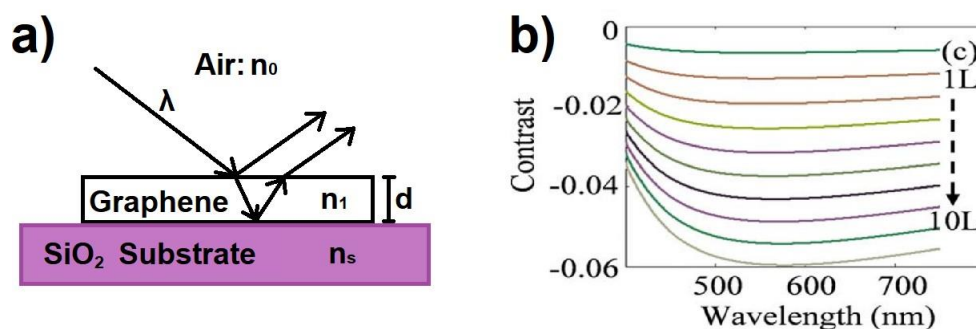
Figure 3.3: Scheme of the interaction between light and graphene over a SiO_2/Si substrate and the optical contrast spectra of ten layer graphene sheet on Si substrate. Retrieved and modified from Teo *et al.* [55] .

The best option to achieve good results by applying an optical contrast method is the use of the software ImageJ (Fiji). Image processing is extremely important in many areas from nanotechnology to astronomy due to its power to analyze optical images. The employment of this software brings many advantages from its open source until the capability to run on any operating system [56]. Among the many functions of ImageJ, we are interested in the analyze particles tool because it is going to provide us the information related to the contrast of a certain sample. This analysis could be achieved and separated in different sections. Thus, it will help us to analyze regions with different number of layers present in the sample of graphene.

In figure 3.4, where the scale bar is a) 100 μm and b) 5 μm, we can appreciate a clear example of the use of
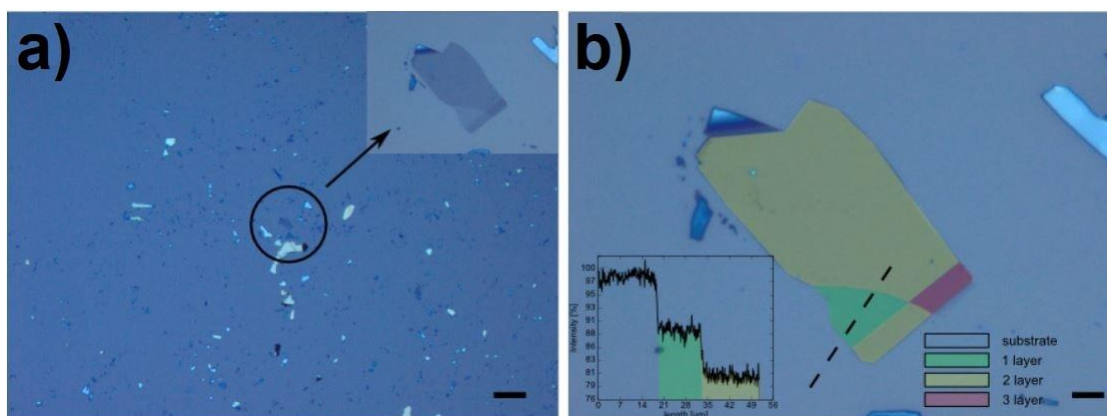
Figure 3.4: a) Overview image of graphite debris on Si/SiO$_2$ substrate. b) false color image indicating the number of layers. Retrieved and modified from Eder [57]

this technique to identify the number of layers of graphene. This examples was taken from Eder [57] , where he first localizes a graphene flake around in the sample as observed in figure 3.4a. A graphene flake with different number of layers is presented in figure 3.4b. Here, it is observed a false color image representing the contrast difference with respect to the background. A similar process is going to be applied in this work and present in the later section.

3.4 Raman Spectroscopy

Among the various techniques that are utilized for the characterization of carbon-based materials, Raman spectroscopy is the most famous. This is mainly due to its amazing ability to understand the behavior of electrons and phonons in graphene. Fundamentally, monochromatic radiation with a certain frequency v_0 interacts with molecules, where the radiation scattered is dispersed leading to reproduce not only the initial frequency v_0 called Rayleigh scattering. Instead, appears a new pair of frequencies in the form of $v_0 \pm v_M$. Thus, Raman scattering, attributed to the first person to observe this phenomenon, is this light scattering with a frequency shift. [58] The composition of these frequencies, or Raman bands is called the Raman spectra. Additionally, these frequencies could be given in the next form:

$$v = v_0 + v_M, \quad v = v_0 - v_M \tag{3.1}$$

However, basic Raman bands are mainly featured by the frequency shift $|v - v_0| = v_M$. Further, there are two processes coupled with the Raman scattering called Stokes and anti-Strokes Raman scattering. In Stokes Raman scattering occurs an upward transition between two molecular energy levels, E_1 and E_2, reaching an energy $hv_M = E_1 - E_2$ and provoking a scattering of lower frequency $v_0 - v_M$. On the contrary, in anti-Stokes Raman scattering we have an inverse process where occurs a downward transition between two molecular energy levels and reaches an energy $hv_M = E_1 - E_2$. This produces a scattering of higher frequency $v_0 + v_M$.
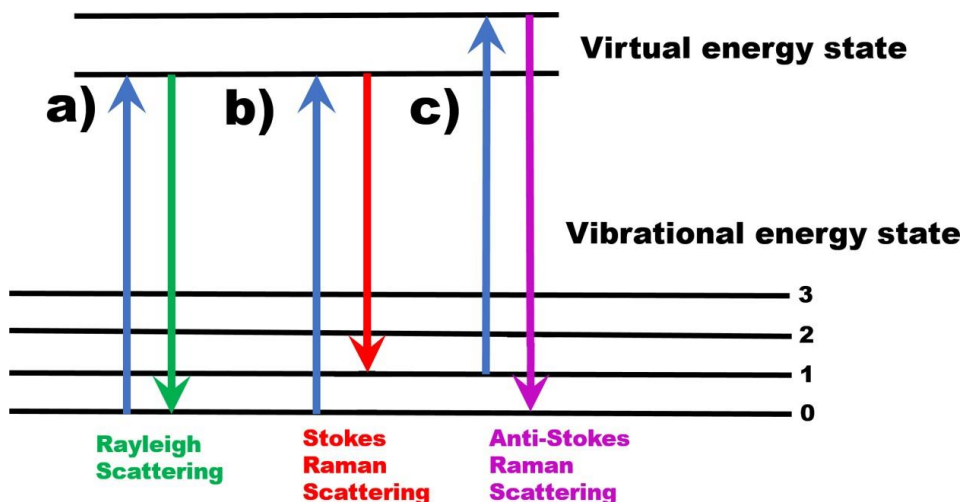
Figure 3.5: Energy-level diagram representing the states involved in the Raman spectra. Figure 3.5a involves an elastic scattering, called Rayleigh scattering, between the photon and the matter. Next, in figure 3.5b and 3.5c, the scattering is seemed to be inelastic scattering, which is based on the loss and gain of energy, respectively. This image was constructed based on Potcoava *et al.* [59].

We can appreciate the three types of scattering present in the Raman spectra in figure 3.5. Basically, the gain/loss of energy will dictate the interaction in the sample when monochromatic light is irradiated to the sample. For example, in figure 3.5a is portraying the Rayleigh scattering, where the scattering does not present a loss or gain of energy i.e. the photon interacts elastically with the matter. On the other hand, if light suffers an inelastic loss of energy, the process involved is called Stokes scattering (see figure 3.5b). In Stokes scattering, the scattered radiation is less than the incident radiation. In the same way, if light suffers a gain of energy, it is called Anti-Stokes scattering as observed in figure 3.5c. On the contrary, the energy of the scattered radiation is higher than the incident irradiation. In general, the Stoke bands are used with more frequency than the Anti-Stokes bands because they involve transitions from lower to higher energy vibrational levels, which means they are more intense [60].

3.4.1   Raman Spectrometer

In general, the equipment required for performing a characterization with Raman spectroscopy is manageable. Firstly, the light source is indispensable for these purposes. Although the first Raman spectra was obtained with the sun as a light source, currently we can use more powerful tools like a laser. [61] Secondly, a detector is required since we need to analyze the scattered light. We necessitate dividing the Raman signals into wavelengths as well. For that purpose, we must use a monochromator, which is not the only device that may help us with that task but it is the simplest. Primarily, the laser passes through a band pass filter, which helps us to reduce the intensity of light. Then,

light crosses a dichroic mirror or Rayleigh filter. This light is focused into an optical microscope where the sample lies. The interaction of the sample with light produces a scattering light and a focusing mirror redirects this light into a long-pass filter. Then, this light passes through the monochromator and goes directly to the detector. In this form, we are able to observe and analyze the shift in frequency of the sample. The scheme of a Raman spectrometer described in this section is shown in figure 3.6a. Furthermore, we can appreciate the real equipment of a Raman spectrometer used to obtain the graphs for this work in figure 3.6b. This equipment remains in the laboratory of Yachay Tech University, which possesses some modern features to increase the efficiency of the data extraction.
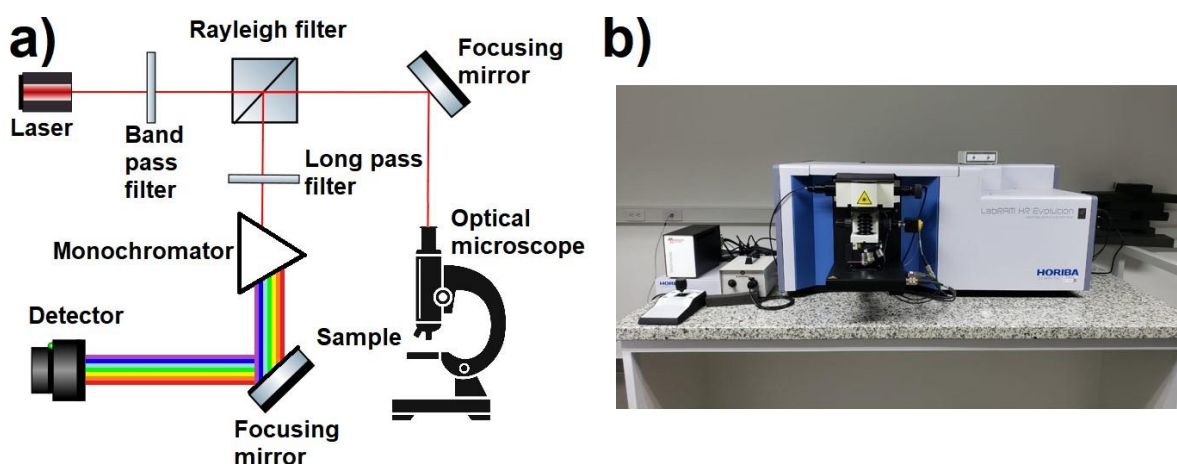
Figure 3.6: a) Scheme of a typical Raman spectrometer. b) Raman spectrometer available at Yachay Tech University used for obtaining of the data.

3.4.2 Raman Spectroscopy for Graphene

In order to interpret the Raman spectra of graphene, we should completely understand its phonon dispersion. For example, we know that single-layer graphene has two carbon atoms in its unit cell, then exists six phonon dispersion bands. Essentially, these bands are divided into two groups with an equal number of bands i.e. three acoustic branches and three optical phonon branches. From this concept, the atomic vibration, of one acoustic branch and for one optical phonon branch, is at 90 degrees to the graphene plane corresponding to the out-of-the-plane phonon modes. On the other hand, the in-plane vibrations correlate with the left two acoustical and optical branches. Usually, these vibrations can occur in the direction of the closest carbon atom, which leads us to classify the phonon modes as longitudinal and transverse. This is thought as the vibrations can take place in perpendicular or parallel to any carbon-carbon directions.[42]

When working with Raman spectroscopy and graphene, we may observe some important characteristics related to single-layer graphene. The G and 2D bands appearing at approximately 1582 cm^{-1} and 2700 cm^{-1}, respectively, are present in graphene where the G band is related to graphite. These features are shown in figure 3.7. The G band is
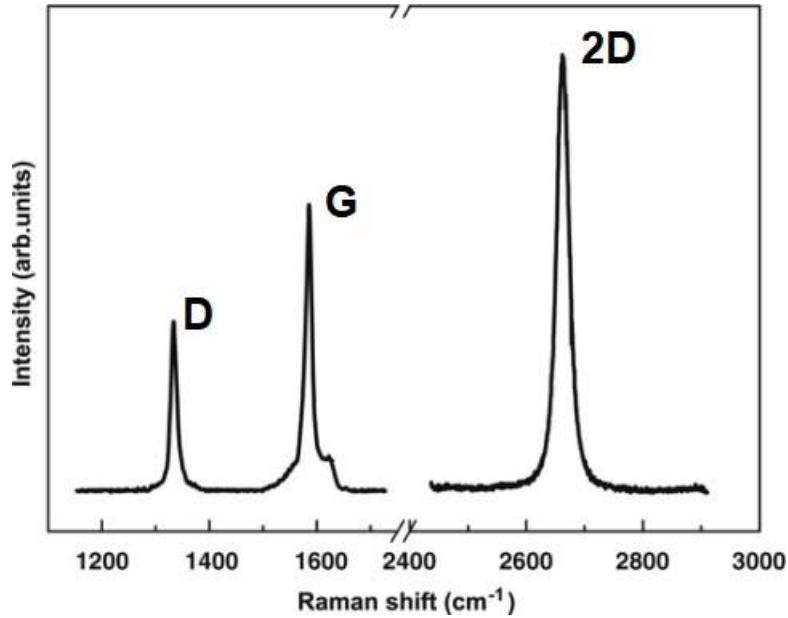
Figure 3.7: Raman spectra of graphene edge with a laser excitation energy of 2.41 eV. Retrieved and modified from Malard *et al.* [42]

truly related to the stretching of sp^2 carbon bonds. In addition, exists another band called disorder-induced D-band, which appears at 1350 cm^{-1}. This band is commonly observed at the edge of graphene or in disordered samples, and it is coupled with the breathing mode of an aromatic ring. [62] Basically, this peak appears when exists defects in the sample. Further, there can be another displaced band called D' band, which exhibits a weaker disorder-induced characteristic at 1620 cm^{-1}. Fundamentally, the doubly degenerate phonon mode at the Brillouin zone is truly associated with the G band. In principle, the 2D and D bands present a dispersive behavior in the frequency owing to a double resonance Raman process (DR). Basically, the wave vectors q of the phonons related to these bands may link preferentially to the electronic states with wavevectors k in the following way q≈2k. [63] An electron of wave vector k around K, and absorbing a photon is the already called DR process. Here, K is the Dirac point, and different initial electronic states around this point altogether with phonons of different symmetries and wave vectors can satisfy the DR condition. [42]

Chapter 4

Results & Discussion

4.1 Graphene Flakes by Mechanical Cleavage

In order to corroborate the objectives proposed in this work, we required the obtaining of graphene flakes. As explained above, the best method to synthesize high-quality graphene flakes is by mechanical cleavage. Although this method presents some issues related to the quantity and number of layers of the intended graphene samples, we can easily perform the optical analysis previously mentioned in order to determine the number of graphene layers.

In this work, the synthesis of graphene by the mechanical cleavage method was attempted. In principle, a few samples of graphene were carried out utilizing this method. However, the samples were observed to be graphene with a large number of layers. Hence, when graphene has numerous layers, it cannot be considered graphene since it has a behavior more like graphite, which implies a change in the intrinsic properties of graphene. Furthermore, two types of tapes, normal scotch tape, and matte acetate tape were used to perform the synthesis. Nevertheless, the normal scotch tape was observed to leave many residuals of the sticky polymer on the substrate. This reduced the visual fields of the graphene samples and cannot be analyzed with the Raman spectrometer. On the other hand, the matte acetate tape presented a better performance in terms of stickiness. This tape had way too much less sticky polymer, which means that the graphene flakes were observable in a better way. Notwithstanding the appreciation range of graphene was higher, the low stickiness of the tape does not allow the extraction of the graphene layers from the HOPG. Indeed, the resulting graphene samples were observed to be graphite instead of multi-layer graphene. As a consequence, the graphene samples presented in this work were not obtained by mechanical cleavage. As an alternative, the characterization and optical contrast analysis were carried out on different graphene samples. This graphene was produced by the CVD method and transferred to a squared substrate on 90 nm SiO_2/Si by a wet process. The results of the experiments performed on this sample are going to be presented next.

4.2   Localization of Graphene Flakes

In order to localize the graphene flakes in the whole sample, we performed an analysis with the Raman spectrometer. Basically, in this process, we use the optical microscope that the Raman spectrometer posses. Then, we try to find some graphene flakes around the sample by dividing the substrate into sections. The tools implemented in the Raman spectrometer facilitate the localization of the graphene flakes since it is easy to control the piezo stage where the graphene sample lies. After that, we can easily find graphene flakes using our "naked eye" principally due to the contrast of the graphene with the SiO_2 substrate. Although this method is commonly used to localize graphene flakes, it cannot help us to determine the number of layers of the graphene sheet. This can be explained by the fact that the optical conditions when performed the experiment can vary from one laboratory to another. Additionally, we can appreciate that this contrast changes according to the number of layers of graphene. In figure 4.1, we can observe that both graphene samples are almost indistinguishable with respect to the substrate. This is mainly related to the absorption of light of graphene because each layer of graphene of a thickness ≈ 0.335 nm absorbs approximately 2.3% of an incident visible light [64]. Besides, this percentage of absorption of light of monolayer graphene scale linearly with the increase of layers on top of graphene. This means that each extra layer of graphene will absorb an additional 2.3% percentage of light. For example, in the case of bilayer graphene, the total light absorbed will be $\approx 4.6\%$ of visible light. The reflectance of graphene also helps in the contrast analysis because it is negligible with approximately less than 0.1%. It is extremely important to mention that both images in figure 4.1 were taken with a magnification of 5x in the microscope. However, the inset images, where we can appreciate better the graphene flake, were taken with a magnification of 100x in order to visualize without effort the graphene flakes. Here, figure 4.1a corresponds to the graphene sample 01 and 4.1b corresponds to graphene sample 02. Both images were carried out on the optical microscope inside the Raman spectrometer, where the magnification can be modulated. In general, exists a few standardized magnifications that are included in the majority of microscopes, where they can magnify until 4, 10, and 40 times their actual size. Nevertheless, this equipment requires an additional magnification owing to the fact that we need to observe and analyze smaller specimens than the conventional samples. In our specific case, we are working with graphene samples which imply the use of greater magnifications because our graphene samples are around 100 μm. Fundamentally, the part of the microscope that enhances the magnification of an image is the objective lens. The objective lens is probably the most important component of the microscope for the reason that it helps us to magnify the image. This happens because of an arrangement of lenses inside the objective that makes us easier to observe a small sample. Hence, there are two main factors that affect the final image, the magnification, and the numerical aperture. Therefore, we can implement two new concepts, resolution and brightness. These two are truly related to the magnification and numerical aperture, respectively. As a consequence, a good objective lens will be dictated by its maximum resolution with relatively good brightness over the sample [65].
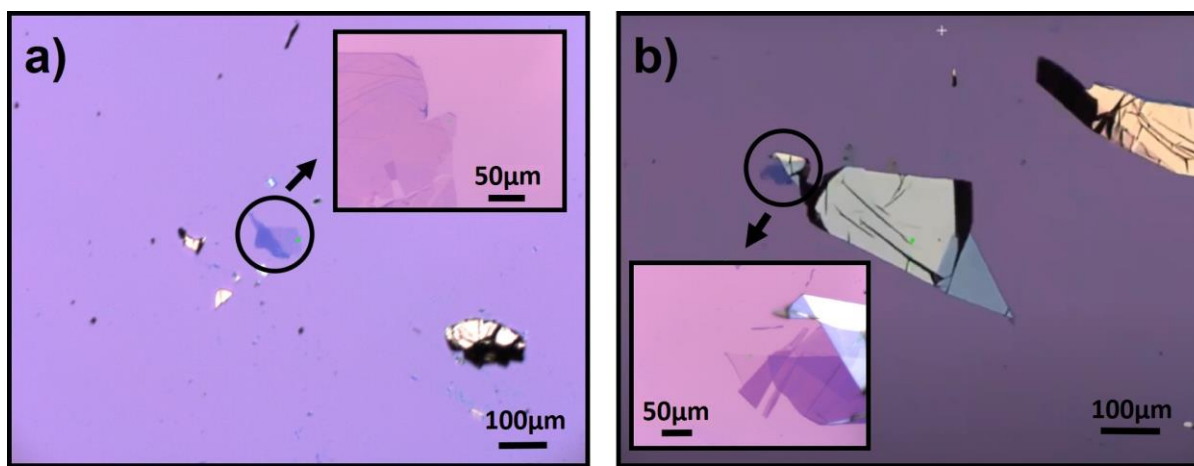
Figure 4.1: Two different graphene samples observed under an optical microscope at 5x magnification, and two inset images corresponding to the graphene samples taken at 100x.

4.3 Optical Contrast Analysis Using ImageJ

The determination of the number of layers of graphene can be easily done by applying a contrast analysis of the samples. The software ImageJ (1.51v) is a useful tool that may help us to perform this analysis since the work with contrast images, and its related processes are able to be done in this software. Therefore, in order to obtain the number of layers of our graphene sample, we require to upload the image taken from the optical microscope. This image was taken by the CCD camera with an aperture of 500 nm incorporated in the Raman spectrometer. Once the image was uploaded to the software, we need to convert this image into an 8-bit version i.e. to change from color to a grayscale image. This procedure is going to help us to effortlessly identify the gray values of the image. Then, the process "analyze particles", which is inside the software, is the one that gives us the gray values. However is very important to adjust a threshold in the image, it means that we are going to select just the graphene flakes in order to analyze them. In the toolbox of set measurements, we can choose the parameters we want to measure in our selected area. For our case, we are going to select the mean gray value. After that, we can observe the displayed list of the gray values. By analyzing these values, we can determine the number of graphene layers as mentioned above. This is due to the contrast of the graphene with the substrate, then the gray values must change with respect to the number of layers. The contrast analysis was performed over two graphene samples, which are described and shown below. We have divided the graphene samples iton 01 and 02. They are divided into regions according to their number of layers, which are related to the contrast difference values obtained.

In figure 4.2, we can appreciate the different regions of the graphene sample 01. In this figure, we can observe how this sample is composed of flakes with a dissimilar number of layers. Therefore, we can mention that a single sample of graphene does not always has the same number of layers. This is mainly attributed to the synthesis method to produce graphene. Although in the majority of cases the graphene samples will always be produced

with a combination of several layers, this sample was synthesized by the CVD growth method among high-quality conditions. In figure 4.2a, we can appreciate that there are a lot of mono-layer graphene regions on the graphene sample. Besides, we have regions with two, three, and four layers of graphene and region 13 are the only one with 4 layers. In figure 4.2a, we also have traced two dashed lines representing the plot profile over this path. Figure 4.2b shows the plot of the contrast values obtained from the path in figure 4.2a. The contrast values plotted in figure 4.2b, which are shown in table 4.1, were calculated using equation 1.4. This equation will help us to calculate the contrast difference value for later compare it with theoretical values. In both tables 4.1 and 4.2, the mean gray values and the standard deviation were extracted with the help of ImageJ. In this case, we have calculated and compared with the studies performed by Li *et al.* [48]. In this study, they carried out the experiment to calculate the number of layers and checked their results with Raman spectroscopy. We can appreciate an error in figure 4.2b at the shift of regions from 1 to 7. The results showed us that region 7 should be mono-layer graphene since the contrast difference value is approximately close to -10.4. Nevertheless, the resulting mean value is -13.694, which makes us think that the error must be related to the optical contrast of the image itself. Another typical factor related to this error is based on the presence of impurities in the sample that impedes the visibility of the graphene sample. Additionally, the peaks observed in figure 4.2b corresponds to the edge of the crystals because there is a higher concentration of graphene.

Figure 4.2: a) False color image from graphene sample 01 showing the number of layers according to their regions and contrast, and b) contrast profile of the dashed line with respect to their color of the graphene flake on SiO_2/Si substrate.

Proceeding to the graphene sample 02 shown in figure 4.3, we did the same experimental procedure where we obtained the contrast difference values. In the same way as before, we can appreciate different graphene flakes with a dissimilar number of layers. Although this graphene sample was supposed to be mono-layer graphene, we can appreciate that these samples present flakes with a number of the layer from 1 to 6 in figure 4.3a. Further, we can appreciate that region 13 is graphite, which can be identified with ease since its a white region. In contrast with

graphene sample 01, this graphene was more easily observed and differentiated the regions with a various number of layers. These results were analyzed according to the theoretical values observed in Li *et al.* [48] . Two dashed lines with different colors were traced over different regions as well, and they can be observed in figure 4.3b. In table 4.2, we can observe the values obtained with the help of the software ImageJ (1.51v) and were calculated using equation 1.4 as well. As an additional fact, the ImageJ software allows us to determine the standard deviation of the mean gray values. We can appreciate that in table 4.1 the standard deviation values are higher than in table 4.2. In general, the data obtained from graphene sample 01 seems to be a little unstable according to the original regions. The Raman spectra in figure 4.4c and 4.4a show us the presence of mono-layer graphene over regions 1 in both cases. However, the other regions, where the mono-layer of graphene lied, were unstable and with higher errors when compared with the data from Li *et al.* [48] . This is shown in table 4.1 where the majority of the standard deviation values are higher. On the contrary, table 4.2 shows low standard deviation values in compared with table 4.1.
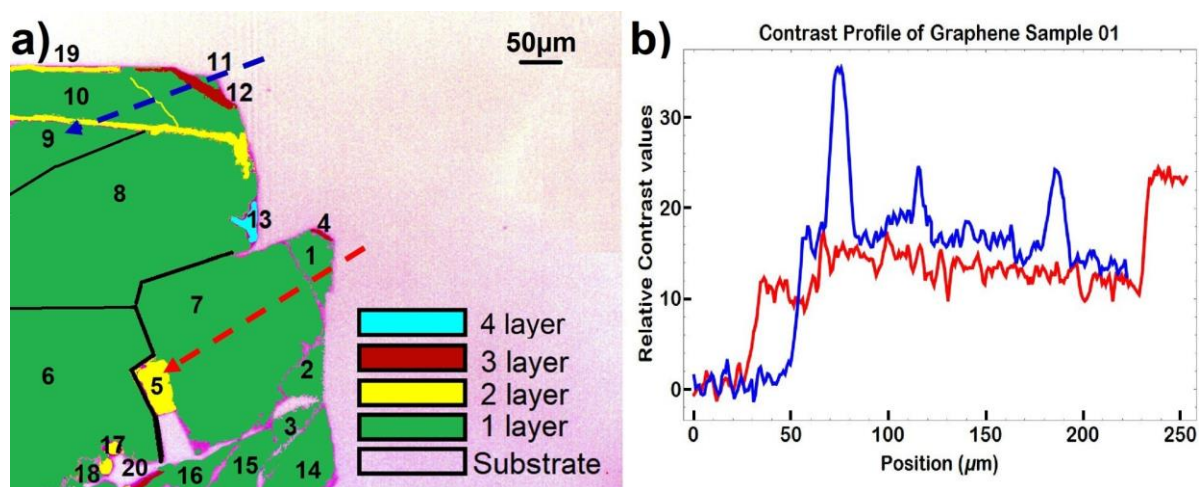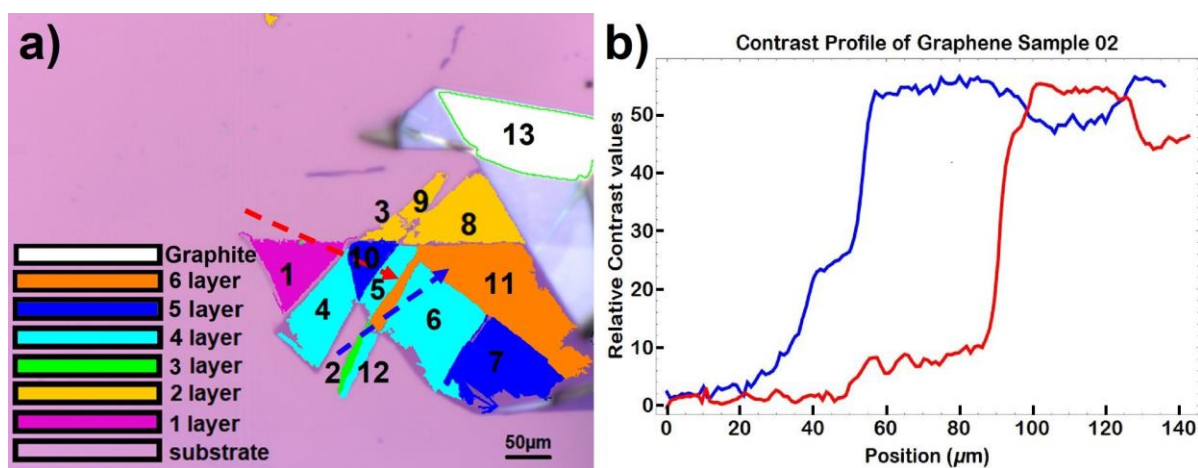

Figure 4.3: False color image from graphene sample 02 showing the number of layers according to their regions and contrast, and b) contrast profiles of the dashed lines with respect to their color of the graphene flake on SiO_2/Si substrate.

Region	Gray values (C_G)		Contrast difference (C_D)	Number of layers
	Mean value (a.u.)	Standard deviation	$C_D = C_G - C_S$ (a.u.)	
1	182.478	1.379	−9.680	1
2	185.243	0.908	−6.915	1
3	185.640	1.397	−6.518	3
4	165.778	2.438	−26.380	2
5	169.766	1.293	−22.392	1
6	182.347	1.178	−9.811	1
7	178.464	1.348	−13.694	1
8	179.709	1.049	−12.449	1
9	185.235	0.972	−6.923	1
10	183.486	1.188	−8.672	1
11	181.333	0.963	−10.825	3
12	161.727	1.689	−30.431	5
13	136.290	3.607	−55.868	1
14	179.643	1.186	−12.515	2
15	180.079	1.306	−12.079	1
16	180.361	2.072	−11.797	1
17	173.188	1.03	−18.970	2
18	185.938	1.063	−6.220	1
19	175.550	1.146	−16.608	2
20	160.346	3.815	−31.812	3
C_S	192.158	1.033	0	0

Table 4.1: Listed values of the mean gray values, contrast difference and number of layers obtained from the experimental data of the graphene sample 01.

Region	Gray values (C_G)		Contrast difference (C_D)	Number of layers
	Mean value (a.u.)	Standard deviation	$C_D = C_G - C_S$ (a.u.)	
1	182.185	0.914	−9.030	1
2	159.250	2.062	−31.965	3
3	168.500	1.291	−22.715	2
4	143.838	0.906	−47.377	4
5	146.188	1.120	−45.027	4
6	140.667	1.049	−50.548	4
7	134.250	0.926	−56.965	5
8	164.312	1.702	−26.903	2
9	166.381	1.987	−24.834	2
10	136.818	0.751	−54.397	5
11	126.275	0.695	−64.940	6
12	144.312	1.887	−46.903	4
C_S	191.215	1.160	0	0

Table 4.2: Listed values of the mean gray values, contrast difference and number of layers obtained from the experimental data of the graphene sample 02.

4.4   Raman Spectroscopy Analysis

The characterization of graphene via Raman spectroscopy was also carried out in this work. In principle, the identification of the number of layers of the graphene samples is difficult. However, we performed a Raman spectroscopy analysis in order to localize mono-layer graphene because this technique could be very useful to differentiate mono-layer from multi-layer graphene. Even so, Raman spectroscopy requires the use of complicated equipment, it is considered a quick and non-destructive technique to analyze graphene samples. Besides, the characterization of the electronic properties of graphene is performed among the wavelength range of 800-3000 cm^{-1}. For this reason, there were meant to be found three major peaks on the Raman spectra located at approximately 1350, 1580, and 2700 cm^{-1}, which are called D, G, and 2D bands, respectively. As we mentioned before, the G band is associated with the E_{2g} phonon at the Brillouin zone center. The D band, also call the disorder-induced band, is present in the graphene Raman spectra representing the concentration of defects in the sample. A 2D peak is the second order of the D peak and is caused by the double resonant Raman scattering with two-phonon emissions[66]. Additionally, is very important to observe the 2D peak in this spectra since this peak is sensitive to the number of layers present in this sample. In general, the intensity and shape of this peak are going to tell us information related to the thickness of graphene. If the intensity of the 2D peak is higher with respect to the G band and the peak is narrowed, we are analyzing a mono-layer graphene sample. We can appreciate this feature and differentiate mono-layer graphene from multi-layer graphene in figure 1.7. That being the case, we can observe three Raman spectra of three regions among the two graphene samples in figure 4.4. For our purposes, the Raman spectroscopy technique was employed to confirm the number of layers present in the sample. Figure 4.4c and figure 4.4a shown the spectra of the graphene sample 01 over the region 1 and 2, respectively. In both images, we can observe that the intensity of the 2D band peak is higher than the G band peak and that the 2D band peak is more prominent and narrowed, which implies a single layer of graphene in this region. Furthermore, we can observe the presence of a D' peak in figure 4.4c and can be attributed to defects present in graphene synthesized by the CVD growth method. A relatively high intense D band peak is present in this spectra as well, implying the presence of defects in the graphene sample. In contrast with the spectra in figure 4.4c, there is not the D' peak in the spectra 4.4a nor 4.4b. This is due to the absence of defects in the graphene flakes. As a matter of fact, the spectra 4.4a has a small D band peak, and spectra 4.4b does not even have a D band peak. Moreover, the three spectra observed in figure 4.4 presented a weak D+D" peak at 2500 cm^{-1}. The Raman spectra shown in figure 4.4b was taken on graphene sample 02 over region 1. In the same way as before, the 2D band peak is more prominent and narrowed, which leads us to conclude that there is mono-layer graphene in this region. This is related to the full width at half maximum of the peak (FWHM), which is the width of the peak. Basically, the response of the 2D band peak according to their number of layers can be explained by the double-resonant Raman model[66]. In the three spectra presented, we can observe three recognizable peaks located at approximately 400, 500, and 950 cm^{-1}, being the peak at 500 cm^{-1} the highest one. These peaks are related to the substrate where graphene samples were lying. In this case, these peaks are a fingerprint of SiO_2/Si substrate and seem to appear in every Raman analysis, then it should be always considered when working on it. These results confirmed the validity of this simplistic method to determine the number of layers of a graphene flake.

Afterwards, we can observe the peak positions of the bands presented in the Raman spectra in figure 4.4 in table
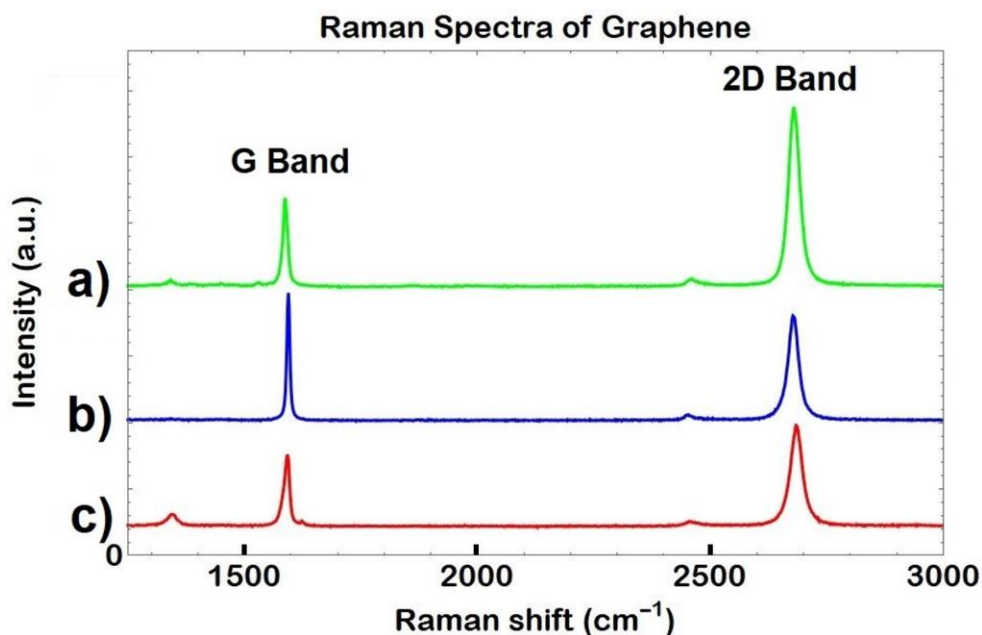
Figure 4.4: Three different Raman spectra a), b), and c) over monolayer graphene and obtained from the two graphene samples in different regions.

4.3. Here, we can associate each sample to the spectra shown above as Gr01 as figure 4.4c, Gr02 as figure 4.4b, and Gr03 as figure 4.4a. Hence, we can observe that the peak positions of the D band in the graphene samples are almost equal. However, we can appreciate a shift of the peak position mainly due to the different excitation laser frequencies that could be occurred during the measurements.   This takes place because of the the D band is a resonant band that exhibits a dispersive behavior [67]. Next, we have the G band, which the peak position is sensitive to the layers present in the sample. As expected, the peak positions in all of the samples are around the same values since we have mono-layer graphene. Finally, The peak positions of the 2D bands are also similar, which again is due to the presence of mono-layer graphene. As a final statement, we can compare these values to the literature mentioned above, and observer that they are almost identical.

	Peak position (cm^{-1})		
	D Band	G Band	2D Band
Gr01	1345.17	1592.38	2683.54
Gr02	1341.99	1593.92	2676.79
Gr03	1341.99	1587.75	2678.14

Table 4.3: Listed values of the peak positions of the principal bands analyzed in the Raman spectra shown above (Fig 4.4).

Chapter 5

Conclusions & Outlook

Although the synthesis of high-quality graphene by applying the mechanical exfoliation technique was the main goal of this work, the graphene samples could not be used for the optical contrast analysis. The principal issue was related with the quality of the sample and the excessive number of layers present in the graphene flakes. Hence, the employment of graphene samples obtained from other sources was required in order to keep going with the experiments. As a consequence, the graphene samples obtained were produced by the CVD growth method, which does not seem to interfere with the goals proposed. Therefore, the experiments and analysis were performed over this graphene sample, which showed very good results.

Once we had the graphene samples, we proceeded to look for a very detailed and differential graphene flake. This procedure was achieved effortlessly with the help of an optical microscopy, which was incorporated inside the Raman spectrometer. For this work, we analyzed two different graphene flakes that were thought to be a composition of different thicknesses. The major problem was to find mono-layer graphene because the contrast of this flake is almost indistinguishable with the substrate. This could be easily accomplish by observing it with "naked eye", however a Raman spectroscopy analysis was performed over the two graphene samples. These analysis confirmed the existence of mono-layer graphene as expected, but in the whole sample there were graphene flakes with higher number of layers. The contrast of the region was the key to interpret the appearance of graphene flakes with more than one layer.

The Raman analysis of the two graphene samples, which were taken over three different regions, was achieved as well. This analysis helped us not only to distinguish the number of layers of graphene but the characterization of the samples. The Raman spectra shown in the results were of great aid to characterize the samples. All the details are described in the previous chapter, but we can stand out two main peaks in the spectra, D and 2D. The D band peak, which is the peak that describes the intensity of defects present in the sample, is almost minimum in the samples. This feature is truly related to the high-quality of the graphene where we performed the analysis. The 2D band is observed similar in all the three spectra, narrowed and well defined, due to the presence of the mono-layer graphene. Nevertheless, one of the spectra shows a D' peak that is associated with the CVD growth method.

The graphene samples were observed under the optical microscope included in the Raman equipment. When

localized the graphene flakes, we took an image that will help us to carry out an optical contrast analysis. This analysis can be done with ease by making the use of the ImageJ (1.51v). This software is a powerful tool in the field of image processing, which came out really good for our purposes. Then, we required to take an image of the samples for after upload it into the program. We can easily set the measurements we want to analyze and extract it from each region of the image. For our case, the mean gray value was necessary to calculate the contrast difference using equation (1.4). As an additional fact, this software allowed us the possibility to obtain the standard deviation in each measure, which is also shown in the results. In principle, the errors of both images are relatively low according to their contrast difference. However, when comparing both samples, we can observe that the standard deviation values of the graphene sample 01 are higher than the values in graphene sample 02.

This work was principally focused on the identification of the number of layers of a graphene flake. The method to reach this objective was the optical contrast analysis, which has some advantages over other methods. This technique allow us the possibility of determine the thickness of graphene without the employment of complicated and expensive equipment. As a matter of fact, the software use to extract all the experimental data is an open source software, which gives the facility for every person to manipulate it. Although the data obtained could present some errors, the results were very well approximated with respect to the values compared. For a future work, the process can be enhanced with the combination of this method with another techniques. For example, the implementation of Raman spectroscopy with optical contrast, where the reflection and transmission could enable the measurement of the full spectrum over the whole range. In this way, the results obtained will be more accurate concerning the exact number of layers in each region of the sample. Nevertheless, the addition of complex equipment could no be easily for all the scientist working on this area.

Bibliography

[1] Hazen, R. M.; Downs, R. T.; Jones, A. P.; Kah, L. Carbon mineralogy and crystal chemistry. *Reviews in Mineralogy and Geochemistry* **2013**, *75*, 7–46.

[2] Geim, A. K.; Novoselov, K. S. *Nanoscience and technology: a collection of reviews from nature journals*; World Scientific, 2010; pp 11–19.

[3] Peschel, G. Carbon-carbon bonds: hybridization. *Obtained online from: http://www. physik. fu-berlin. de/einrichtungen/ag/ag-reich/lehre/Archiv/ss2011/docs/Gina_Peschel-Handout. pdf, published on* **2011**, *5*.

[4] Avouris, P.; Dimitrakopoulos, C. Graphene: synthesis and applications. *Materials today* **2012**, *15*, 86–97.

[5] Kumar, S.; Saeed, G.; Zhu, L.; Hui, K. N.; Kim, N. H.; Lee, J. H. 0D to 3D carbon-based networks combined with pseudocapacitive electrode material for high energy density supercapacitor: A review. *Chemical Engineering Journal* **2021**, *403*, 126352.

[6] Smalley, R. E. Discovering the fullerenes. *Reviews of Modern Physics* **1997**, *69*, 723.

[7] Wudl, F. Fullerene materials. *Journal of Materials Chemistry* **2002**, *12*, 1959–1963.

[8] Choho, K.; Langenaeker, W.; Van De Woude, G.; Geerlings, P. Reactivity of fullerenes. Quantum-chemical descriptors versus curvature. *Journal of Molecular Structure: THEOCHEM* **1995**, *338*, 293–301.

[9] Ahmad, S. Carbon nanostructures fullerenes and carbon nanotubes. *IETE Technical Review* **1999**, *16*, 297–310.

[10] Dresselhaus, M. S.; Dresselhaus, G.; Eklund, P. C. *Science of fullerenes and carbon nanotubes: their properties and applications*; Elsevier, 1996.

[11] Sola, M.; Mestres, J.; Duran, M. Molecular size and pyramidalization: two keys for understanding the reactivity of fullerenes. *The Journal of Physical Chemistry* **1995**, *99*, 10752–10758.

[12] Wilder, J. W.; Venema, L. C.; Rinzler, A. G.; Smalley, R. E.; Dekker, C. Electronic structure of atomically resolved carbon nanotubes. *Nature* **1998**, *391*, 59–62.

[13] Eatemadi, A.; Daraee, H.; Karimkhanloo, H.; Kouhi, M.; Zarghami, N.; Akbarzadeh, A.; Abasi, M.; Hanifeh-pour, Y.; Joo, S. W. Carbon nanotubes: properties, synthesis, purification, and medical applications. *Nanoscale research letters* **2014**, *9*, 1–13.

[14] Grobert, N. Carbon nanotubes–becoming clean. *Materials today* **2007**, *10*, 28–35.

[15] Su, M.; Zheng, B.; Liu, J. A scalable CVD method for the synthesis of single-walled carbon nanotubes with high catalyst productivity. *Chemical physics letters* **2000**, *322*, 321–326.

[16] Dresselhaus, M. S.; Dresselhaus, G.; Sugihara, K.; Spain, I. L.; Goldberg, H. A. *Graphite fibers and filaments*; Springer Science & Business Media, 2013; Vol. 5.

[17] Yakobson, B. I.; Avouris, P. Mechanical properties of carbon nanotubes. *Carbon nanotubes* **2001**, 287–327.

[18] Lekawa-Raus, A.; Patmore, J.; Kurzepa, L.; Bulmer, J.; Koziol, K. Electrical properties of carbon nanotube based fibers and their future use in electrical wiring. *Advanced Functional Materials* **2014**, *24*, 3661–3682.

[19] Tiwari, S. K.; Kumar, V.; Huczko, A.; Oraon, R.; Adhikari, A. D.; Nayak, G. Magical allotropes of carbon: prospects and applications. *Critical Reviews in Solid State and Materials Sciences* **2016**, *41*, 257–317.

[20] Terrones, M. Science and technology of the twenty-first century: synthesis, properties, and applications of carbon nanotubes. *Annual review of materials research* **2003**, *33*, 419–501.

[21] Geis, M.; Efremow, N.; Rathman, D. Device applications of diamonds. Ph.D. thesis, American Vacuum Society, 1988.

[22] Robertson, J. Properties of diamond-like carbon. *Surface and Coatings Technology* **1992**, *50*, 185–203.

[23] Belenkov, E.; Greshnyakov, V. Structure, properties, and possible mechanisms of formation of diamond-like phases. *Physics of the Solid State* **2016**, *58*, 2145–2154.

[24] Djurišić, A. B.; Li, E. H. Optical properties of graphite. *Journal of applied physics* **1999**, *85*, 7404–7410.

[25] Chung, D. Review graphite. *Journal of materials science* **2002**, *37*, 1475–1489.

[26] Taft, E.; Philipp, H. Optical properties of graphite. *Physical Review* **1965**, *138*, A197.

[27] Inagaki, M. Applications of graphite intercalation compounds. *Journal of Materials Research* **1989**, *4*, 1560–1568.

[28] Li, X.; Zhi, L. Graphene hybridization for energy storage applications. *Chemical Society Reviews* **2018**, *47*, 3189–3216.

[29] Dresselhaus, M. S.; Araujo, P. T. Perspectives on the 2010 nobel prize in physics for graphene. 2010.

[30] Huang, M.; Yan, H.; Chen, C.; Song, D.; Heinz, T. F.; Hone, J. Phonon softening and crystallographic orientation of strained graphene studied by Raman spectroscopy. *Proceedings of the National Academy of Sciences* **2009**, *106*, 7304–7308.

[31] Bullock, C. J.; Bussy, C. Biocompatibility considerations in the design of graphene biomedical materials. *Advanced Materials Interfaces* **2019**, *6*, 1900229.

[32] McCann, E. Asymmetry gap in the electronic band structure of bilayer graphene. *Physical Review B* **2006**, *74*, 161403.

[33] Zhang, Z.; Chang, K.; Peeters, F. Tuning of energy levels and optical properties of graphene quantum dots. *Physical review B* **2008**, *77*, 235411.

[34] Xia, F.; Mueller, T.; Lin, Y.-m.; Valdes-Garcia, A.; Avouris, P. Ultrafast graphene photodetector. *Nature nanotechnology* **2009**, *4*, 839–843.

[35] Falkovsky, L. A. Optical properties of graphene and IV–VI semiconductors. *Physics-Uspekhi* **2008**, *51*, 887.

[36] Mecklenburg, M.; Schuchardt, A.; Mishra, Y. K.; Kaps, S.; Adelung, R.; Lotnyk, A.; Kienle, L.; Schulte, K. Aerographite: ultra lightweight, flexible nanowall, carbon microtube material with outstanding mechanical performance. *Advanced Materials* **2012**, *24*, 3486–3490.

[37] Frank, I.; Tanenbaum, D. M.; van der Zande, A. M.; McEuen, P. L. Mechanical properties of suspended graphene sheets. *Journal of Vacuum Science & Technology B: Microelectronics and Nanometer Structures Processing, Measurement, and Phenomena* **2007**, *25*, 2558–2561.

[38] Pop, E.; Varshney, V.; Roy, A. K. Thermal properties of graphene: Fundamentals and applications. *MRS bulletin* **2012**, *37*, 1273–1281.

[39] Nihira, T.; Iwata, T. Temperature dependence of lattice vibrations and analysis of the specific heat of graphite. *Physical Review B* **2003**, *68*, 134305.

[40] Dresselhaus, M. S.; Dresselhaus, G. Intercalation compounds of graphite. *Advances in physics* **2002**, *51*, 1–186.

[41] Novoselov, K. S.; Geim, A. K.; Morozov, S. V.; Jiang, D.-e.; Zhang, Y.; Dubonos, S. V.; Grigorieva, I. V.; Firsov, A. A. Electric field effect in atomically thin carbon films. *science* **2004**, *306*, 666–669.

[42] Malard, L.; Pimenta, M. A.; Dresselhaus, G.; Dresselhaus, M. Raman spectroscopy in graphene. *Physics reports* **2009**, *473*, 51–87.

[43] Whitener Jr, K. E.; Sheehan, P. E. Graphene synthesis. *Diamond and related materials* **2014**, *46*, 25–34.

[44] Liu, J.; Liu, Z.; Barrow, C. J.; Yang, W. Molecularly engineered graphene surfaces for sensing applications: A review. *Analytica chimica acta* **2015**, *859*, 1–19.

[45] Punckt, C.; Pope, M. A.; Liu, J.; Lin, Y.; Aksay, I. A. Electrochemical performance of graphene as effected by electrode porosity and graphene functionalization. *Electroanalysis* **2010**, *22*, 2834–2841.

[46] Li, Z.-Y.; Akhtar, M. S.; Kuk, J. H.; Kong, B.-S.; Yang, O.-B. Graphene application as a counter electrode material for dye-sensitized solar cell. *Materials Letters* **2012**, *86*, 96–99.

[47] Zhang, H.; Tang, D.; Zhao, L.; Bao, Q.; Loh, K. Large energy mode locking of an erbium-doped fiber laser with atomic layer graphene. *Optics Express* **2009**, *17*, 17630–17635.

[48] Li, H.; Wu, J.; Huang, X.; Lu, G.; Yang, J.; Lu, X.; Xiong, Q.; Zhang, H. Rapid and reliable thickness identification of two-dimensional nanosheets using optical microscopy. *ACS nano* **2013**, *7*, 10344–10353.

[49] Xu, K.; Cao, P.; Heath, J. R. Graphene visualizes the first water adlayers on mica at ambient conditions. *Science* **2010**, *329*, 1188–1191.

[50] Li, H.; Lu, G.; Yin, Z.; He, Q.; Li, H.; Zhang, Q.; Zhang, H. Optical identification of single-and few-layer MoS2 sheets. *Small* **2012**, *8*, 682–686.

[51] Calizo, I.; Bejenari, I.; Rahman, M.; Liu, G.; Balandin, A. A. Ultraviolet Raman microscopy of single and multilayer graphene. *Journal of applied physics* **2009**, *106*, 043509.

[52] Davidson, M. W.; Abramowitz, M. Optical microscopy. *Encyclopedia of imaging science and technology* **2002**, *2*, 120.

[53] Zhang, Y.; Tan, Y.-W.; Stormer, H. L.; Kim, P. Experimental observation of the quantum Hall effect and Berry's phase in graphene. *nature* **2005**, *438*, 201–204.

[54] Blake, P.; Hill, E.; Castro Neto, A.; Novoselov, K.; Jiang, D.; Yang, R.; Booth, T.; Geim, A. Making graphene visible. *Applied physics letters* **2007**, *91*, 063124.

[55] Teo, G.; Wang, H.; Wu, Y.; Guo, Z.; Zhang, J.; Ni, Z.; Shen, Z. Visibility study of graphene multilayer structures. *Journal of applied physics* **2008**, *103*, 124302.

[56] Abràmoff, M. D.; Magalhães, P. J.; Ram, S. J. Image processing with ImageJ. *Biophotonics international* **2004**, *11*, 36–42.

[57] Eder, D. I. F. A Microscopic Analysis of Deliberately Introduced Structural Modifications in Free-Standing Graphene.

[58] Long, D. A. Raman spectroscopy. *New York* **1977**, *1*.

[59] Potcoava, M. C.; Futia, G. L.; Aughenbaugh, J.; Schlaepfer, I. R.; Gibson, E. A. Raman and coherent anti-Stokes Raman scattering microscopy studies of changes in lipid content and composition in hormone-treated breast and prostate cancer cells. *Journal of Biomedical Optics* **2014**, *19*, 111605.

[60] Bumbrah, G. S.; Sharma, R. M. Raman spectroscopy–Basic principle, instrumentation and selected applications for the characterization of drugs of abuse. *Egyptian Journal of Forensic Sciences* **2016**, *6*, 209–215.

[61] Graves, P.; Gardiner, D. Practical raman spectroscopy. *Springer* **1989**,

[62] Eda, G.; Chhowalla, M. Chemically derived graphene oxide: towards large-area thin-film electronics and optoelectronics. *Advanced materials* **2010**, *22*, 2392–2415.

[63] Thomsen, C.; Reich, S. Double resonant Raman scattering in graphite. *Physical review letters* **2000**, *85*, 5214.

[64] Li, Q.; Lu, J.; Gupta, P.; Qiu, M. Engineering optical absorption in graphene and other 2D materials: advances and applications. *Advanced Optical Materials* **2019**, *7*, 1900595.

[65] Piston, D. W. Choosing objective lenses: the importance of numerical aperture and magnification in digital optical microscopy. *The Biological Bulletin* **1998**, *195*, 1–4.

[66] Tang, B.; Guoxin, H.; Gao, H. Raman spectroscopic characterization of graphene. *Applied Spectroscopy Reviews* **2010**, *45*, 369–407.

[67] Wall, M. The Raman spectroscopy of graphene and the determination of layer thickness. *Thermo Sci* **2011**, *5*, 1–5.